Reviewed Preprint
v1 • May 30, 2025
Not revised

Reviewed Preprint
v2 • July 23, 2026
Revised by authors

Disruption of sphingolipid metabolism promotes tau seeding through endolysosomal membrane rigidification and rupture

Jessica Tittelmeier[1], Carl Alexander Sandhof[2,3], Nicole Martin[1], Deike El-Kabarity[1], Soki-Bradel Ngonza-Nito[4], Ronald Melki[4], Carmen Nussbaum-Krammer[1,2]

[1]Chair of Neuroanatomy, Institute of Anatomy, Faculty of Medicine, Ludwig-Maximilians University of Munich (LMU), Munich, Germany • [2]Center for Molecular Biology of Heidelberg University (ZMBH) and German Cancer Research Center (DKFZ), DKFZ-ZMBH Alliance, Heidelberg, Germany • [3]Chemical Neurobiology Laboratory, Center for Genomic Medicine, Departments of Neurology and Psychiatry, Massachusetts General Hospital and Harvard Medical School, Boston, United States • [4]Institute Francois Jacob (MIRCen), CEA, and Laboratory of Neurodegenerative Diseases, CNRS, Fontenay-aux-Roses, France

For correspondence: carmen.nussbaum@med.uni-muenchen.de

Competing interests: No competing interests declared

Funding: See page 23

Reviewing editor: Ellen Nollen, University of Groningen, Netherlands

eLife Assessment

This **important** study addresses the role of sphingolipid metabolism in maintaining endolysosomal membrane integrity and its impact on tau pathology in Caenorhabditis elegans and human cell culture models. The findings are **convincing**, and the proposed mechanisms are conceivable. The experimental evidence supports the conclusions of the study. The work will be of broad interest to cell biologists and biologists working on Alzheimer's disease and related proteinopathies.

https://doi.org/10.7554/eLife.106865.2.sa4

Abstract

Endolysosomal dysfunction is a hallmark of Alzheimer's disease (AD) and related tauopathies, yet underlying mechanisms remain poorly understood. This study investigates the role of sphingolipid metabolism in maintaining endolysosomal membrane integrity and its impact on tau aggregation and toxicity in *Caenorhabditis elegans* and human cell culture models. Fluorescence recovery after photobleaching and C-Laurdan dye imaging revealed that silencing sphingolipid metabolism genes reduced endolysosomal vesicle membrane fluidity, increasing their rupture. The accumulation of aggregated tau in endolysosomal vesicles further aggravated endomembrane rigidification and damage and promoted seeded tau aggregation, potentially by facilitating the escape of tau seeds from the endolysosomal system. Supplementation with unsaturated fatty acids improved membrane fluidity, suppressing endolysosomal rupture and seeded tau aggregation in cell models, and alleviating tau-associated neurotoxicity in *C. elegans*. Together, this study provides mechanistic insight into how perturbation of sphingolipid metabolism promotes endolysosomal membrane damage and contributes to the escape of aggregated tau from this compartment, suggesting that restoration of membrane fluidity may represent a strategy to limit tau propagation and toxicity.

Introduction

The gradual accumulation of microtubule-associated protein tau (MAPT/tau) aggregates is a hallmark of Alzheimer's disease (AD) and related tauopathies. Misfolded tau species exhibit prion-like behavior by self-replicating and spreading from cell to cell[1,2]. This contributes to the

progression of pathology and neurotoxicity, eventually culminating in widespread neuronal dysfunction and degeneration[3]. At the molecular level, tau aggregates replicate by templating the conversion of native tau into an amyloid conformation, promoting its accumulation into fibrillar aggregates. For this to occur at the cellular level, seeding-competent tau species (or tau "seeds") must be released from a donor cell and taken up into the cytosol of the neighboring receiving cell in order to come into direct contact with the cytosolic native tau protein[4–6].

In this process, the autophagy-lysosomal pathway (ALP), which is an important clearance route for tau[7], appears to play a central role. Studies have demonstrated impaired ALP function in the brains of tauopathy patients as well as in animal and cell models, showing that the accumulation of abnormal autolysosomal and endolysosomal vesicles correlating with neuronal toxicity[8–11]. Inhibition of autophagic clearance of tau increases its secretion and spreading[12]. In addition, the accumulation of misfolded tau within endolysosomes leads to a destabilization and rupture of these vesicles[13–18]. While intact endolysosomes normally restrict tau seeds from reaching cytosolic monomers, membrane rupture allows their escape. Recent studies highlight this escape as a critical rate-limiting step in seeded tau propagation[13–18]. Endolysosomal damage not only promotes the propagation of pathological aggregates, but also causes the release of hydrolytic enzymes into the cytosol, leading to cellular damage and death[19]. Although recent efforts to identify pathways involved in endolysosomal damage and repair have intensified, many aspects of these processes remain unknown.

To identify cellular factors that are critical for the integrity of endolysosomal vesicles, we recently performed an unbiased genome-wide RNA interference (RNAi) screen in *C. elegans*[20]. One of the pathways identified was sphingolipid (SL) metabolism. SLs constitute a large and diverse class of lipids that are involved in various physiological processes[21, 22]. They consist of two main building blocks, a long-chain base with a serine backbone and an attached long acyl chain. This characteristic chemical structure mediates unique biophysical properties. SL biosynthesis and degradation rely on a specialized enzymatic machinery distinct from that of other lipids[23] (Figure 1A). Functionally, SLs, along with glycerolipids and sterols, serve as structural components of cell membranes, contributing to the stability and fluidity of membranes and to the organization of microdomains such as lipid rafts. Beyond their structural role, SLs serve as bioactive molecules participating in cellular signaling pathways that control cell growth, differentiation, apoptosis, and intercellular communication[24]. Abnormalities in SL metabolism have been observed during aging and in neurodegenerative conditions, including AD, underscoring their potential significance in the pathogenesis of these disorders[25, 26]. Interestingly, recent evidence suggests that sphingolipid accumulation disturbs the endolysosomal pathway and induces or potentiates endolysosomal membrane rupture[27, 28]; however, the mechanisms underlying membrane destabilization remain unclear.

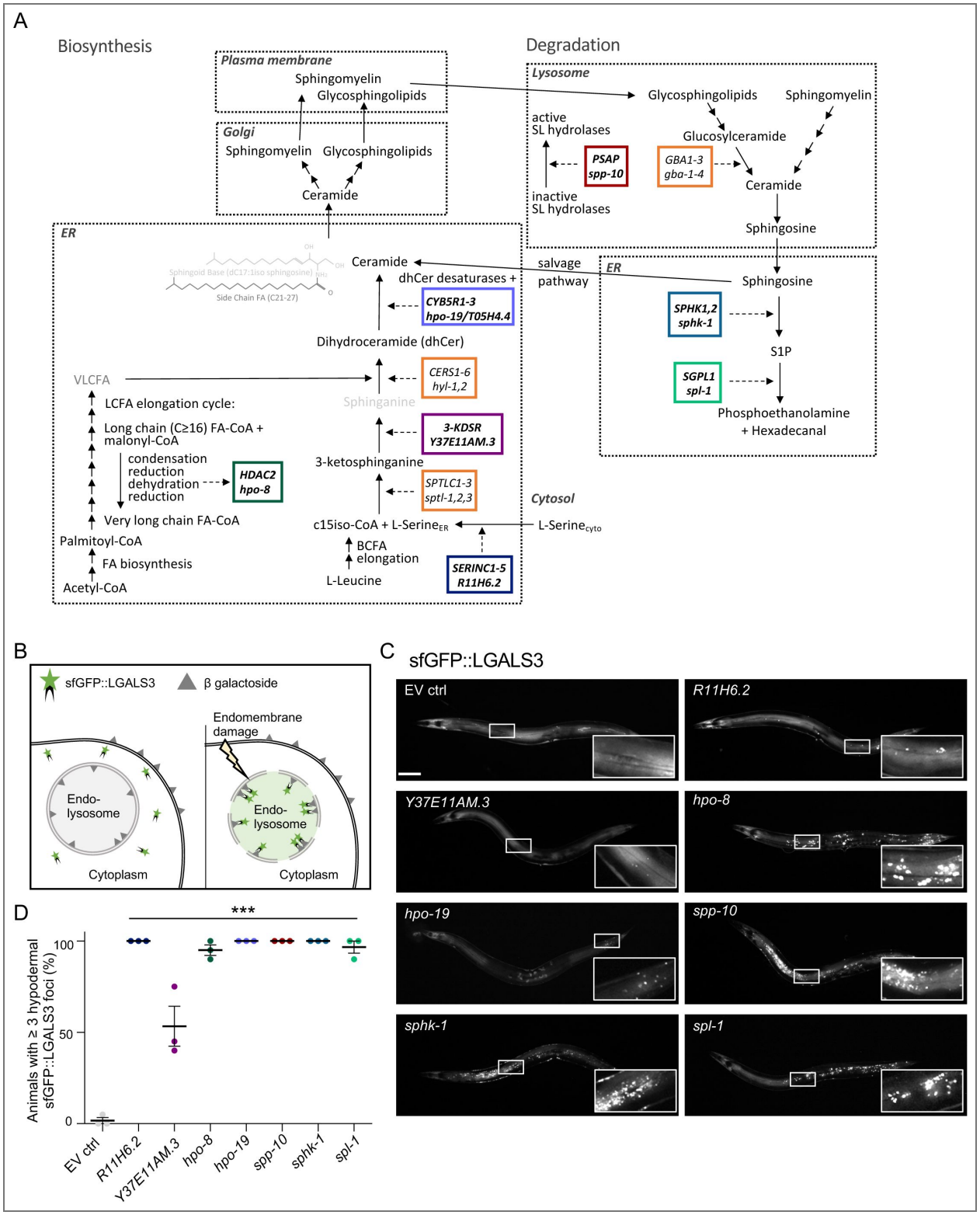

Figure 1. Knockdown of sphingolipid metabolism genes promotes endolysosomal vesicle rupture.

(A) General overview of sphingolipid metabolism with a particular focus on the genes identified in the genome-wide screen. Sphingolipids constitute a group of amphipathic lipids featuring a polar head group and a sphingoid base backbone that is N-acetylated with a (very) long-chain fatty acid ((V)LCFA) side chain. In contrast to mammals, where the sphingoid base is conventionally derived from palmitic acid and serine, *C. elegans* sphingolipids usually contain a

characteristic C17iso branched chain sphingoid base[75–77]. Its synthesis involves the branched chain FA (BCFA) elongation pathway to yield C15iso-CoA, which then condenses with L-serine to form 3-ketosphinganine. This reaction is catalyzed by serine palmitoyltransferase (encoded by *sptl-1*, *-2*, and *-3*). The serine incorporator (SERINC) protein family (encoded by *R11H6.2*) is believed to assist in the incorporation of L-serine into specific membranes. 3-ketodihydrosphingosine reductase (KDSR, in *C. elegans* predicted to be encoded by *Y37E11AM.3*) then catalyzes the reduction of 3-keto sphinganine to sphinganine. The (V)LCFA side chain is primarily comprised of a straight saturated FA chain, ranging from 20-26 carbon atoms in length, with or without hydroxylation[30, 78]. It can also be derived from BCFAs, such as C15iso and C17iso[75, 76]. However, most of the side chain FA moieties originate from palmitoyl-CoA via the canonical de novo FA biosynthesis pathway, involving the sequential addition of C2 moieties from malonyl-CoA through the LCFA elongation cycle[75, 76]. Each elongation cycle comprises four reactions (condensation, reduction, dehydration, reduction), with the third reaction requiring very-long-chain (3R)-3-hydroxyacyl-CoA dehydratase (encoded by *hpo-8*)[76]. Finally, ceramide synthases (encoded by *hyl-1* and *hyl-2*) catalyze the addition of various acyl side chains to the sphingoid base to yield dihydroceramide, which is then desaturated to ceramide. The latter reaction is catalyzed by dihydroceramide desaturases, which require electrons from NAD(P)H provided by cytochrome b5 reductases (encoded by *hpo-19* and *T05H4.4*). All complex sphingolipids, such as sphingomyelin and glycosphingolipids (including cerebrosides and gangliosides) originate from ceramide. Degradation of complex sphingolipids takes place in the lysosome. Essential for this process are saposins or sphingolipid activator proteins (PSAPs, encoded by *spp-10*), which serve as crucial bridges between the lipid substrate and hydrophilic hydrolases. Glucocerebrosidases (encoded by *gba-1*, *gba-2*, *gba-3*, and *gba-4*) hydrolyse glucosylceramide into ceramide and glucose. Sphingosine may be either recycled and metabolized back into ceramide or phosphorylated by sphingosine kinase (encoded by *sphk-1*) to generate sphingosine-1-phosphate (S1P). S1P lyase (encoded by *spl-1*) irreversibly cleaves S1P into phospho-ethanolamine and hexadecenal. The *C. elegans* genes identified in the primary screen, along with their human orthologs, are framed with color. Genes identified in subsequent co-RNAi experiments and their human orthologs are framed in gray. **(B)** Schematic of lysosomal rupture detected by the galectin puncta assay. **(C)** Widefield fluorescence images of day 5 (second day of adulthood) animals expressing F3ΔK281::mCherry in touch receptor neurons and hypodermal sfGFP::LGALS3 and RNAi mediated KD of indicated sphingolipid metabolism genes. Numerous foci are visible indicating lysosomal rupture. Zoomed in image is indicated in overview image by a white box. Scale bar 100 µm. **(D)** Mean percentage of day 5 (second day of adulthood) animals positive for lysosomal rupture (defined as three or more sfGFP::LGALS3 foci in the hypodermis). Data shown as means of three technical replicate plates with 17-30 animals per plate ± SEM. Statistical analysis comparing RNAi conditions to the empty vector control (EV ctrl) was done using one-way ANOVA with Dunnett's post-hoc test. *** = $p < 0.001$.

Here we investigated the role of SL metabolism in maintaining endolysosomal vesicle integrity. Our results revealed that silencing of SL metabolism genes led to a marked reduction in membrane fluidity, particularly in membranes of endolysosomal vesicles, thereby increasing their fragility and susceptibility to rupture. The accumulation of aggregated tau had an additive effect and led to a further reduction in endomembrane fluidity, which aggravated the damage to the endolysosomal compartment. Increased membrane rigidity also facilitated seeded tau aggregation. Conversely, improving membrane fluidity through supplementation with polyunsaturated fatty acids (PUFAs) counteracted tau propagation in cells and tau-associated neurotoxicity in *C. elegans*.

This study highlights the interplay between lipid metabolism and proteostasis and provides insights into how perturbations in sphingolipid metabolism contribute to endolysosomal membrane dysfunction and tau-associated phenotypes. In addition, our data offer a potential mechanistic explanation for the beneficial effects of PUFA-rich diets or PUFA supplementation reported in AD patients and suggest that restoring membrane fluidity may help mitigate tau toxicity and disease progression.

Results

Disruption of sphingolipid metabolism induces endolysosomal rupture

Alterations in SL metabolism are increasingly recognized in aging and neurodegenerative diseases, including AD; however, it remains unclear whether these changes actively contribute to disease pathology or merely reflect downstream consequences of neurodegeneration. In our previously published unbiased genome-wide RNAi screen in *C. elegans*, we identified SL metabolism as one of the pathways whose disruption compromises endolysosomal membrane integrity[20]. Here, we focused on these SL-related hits to better understand how perturbation of SL metabolism promotes endolysosomal rupture and whether it affects tau-related phenotypes.

To first confirm the SL-related hits under the same assay conditions in which they were originally identified, we used the *C. elegans* reporter strain from our previously published screen[20] (Table S1). In this strain, endolysosomal membrane damage is monitored in the hypodermis by expression of human galectin-3 fused to superfolder-GFP (sfGFP::LGALS3). The animals also express an aggregation-prone tau fragment fused to mCherry (F3ΔK281::mCherry) in touch receptor neurons, which is transmitted to the hypodermis, as described previously[20]. Under steady-state conditions, sfGFP::LGALS3 remains diffusely distributed throughout the cytosol. Upon endolysosomal damage, luminal β-galactosides become exposed and recruit sfGFP::LGALS3 into visible puncta, providing a sensitive readout of vesicle rupture[20,29] (Figure 1B).

Using this reporter system, we confirmed that knockdown (KD) of selected SL-related hits increased sfGFP::LGALS3 foci formation. These hits included the serine incorporator *R11H6.2*, the 3-ketodihydrosphingosine reductase *Y37E11AM.3*, the hydroxyacyl-CoA dehydratase *hpo-8*, the cytochrome b5 reductases *hpo-19* and *T05H4.4*, the saposin *spp-10*, the sphingosine kinase *sphk-1*, and the sphingosine-1-phosphate lyase *spl-1* (Figure 1C, D). As genetic validation independent of RNAi, we tested an available *sphk-1* mutant strain, which also showed a robust increase in hypodermal sfGFP::LGALS3 foci (Figure S1A). These data support the conclusion that genetic perturbation of sphingolipid metabolism compromises endolysosomal integrity.

The screen identified distinct steps in sphingolipid metabolism catalyzed by non-redundant genes or targeted by a single RNAi clone, as in the case of *hpo-19*/*T05H4.4* which are both depleted by *hpo-19* RNAi (Figure 1A). However, other steps in this pathway, which are mediated by two or more proteins may have been missed in the screen. Indeed, simultaneous KD of selected redundant genes using co-RNAi revealed additional genes functioning in *de novo* sphingolipid biosynthesis that also induced endolysosomal rupture, including the serine palmitoyltransferases *sptl-1* and *-3* and the ceramide synthases *hyl-1* and *-2* (Figure S1B). In addition, the co-KD of all four glucocerebrosidases *gba-1-4* or only *gba-2-4*, also triggered endolysosomal rupture (Figure S1C). Together, these results indicate that perturbing SL metabolism at multiple steps can compromise endolysosomal integrity, highlighting the tight metabolic balance required to maintain the stability of the endolysosomal limiting membrane. Because KD efficiency was not assessed for the individual RNAi clones or co-RNAi combinations, these experiments do not allow comparison of relative RNAi strength or inference of the relative importance of individual genes. Thus, the conclusions drawn from these RNAi experiments are qualitative: specific single or combined KDs can promote endolysosomal rupture, whereas the absence of a detectable phenotype after RNAi cannot exclude gene involvement, as KD may have been insufficient.

Disruption of sphingolipid metabolism reduces endolysosomal membrane fluidity in *C. elegans*

SLs are important components of eukaryotic cell membranes and genetic modulation of SL metabolism likely affects the lipid composition and biophysical properties of membranes. Similar to their mammalian isoforms, the N-acyl chains of *C. elegans* SLs contain predominantly long and saturated fatty acid chains[30, 31], which tend to pack tightly within the lipid bilayer. As such, a

higher proportion of SLs generally reduces membrane fluidity, leading to increased order, rigidity, or viscosity[32]. Consequently, KD of the hits involved in SL degradation should lead to SL accumulation and reduced membrane fluidity, while KD of the hits involved in SL biosynthesis should have the opposite effect.

To evaluate the membrane fluidity of endolysosomal membranes, fluorescence recovery after photobleaching (FRAP) was employed on *C. elegans* that express the Lysine/Arginine Transporter 1 (LAAT-1) tagged with mCherry, which localizes to the lysosomal membrane[33]. FRAP enables the assessment of the lateral mobility of LAAT-1 within the lysosomal membrane, thereby indirectly measuring its fluidity. We focused our analysis on the hypodermis, where we expressed the sfGFP::LGALS3 reporter and observed endolysosomal rupture following KD of the SL metabolism genes (Figure 1C, D). Interestingly, KD of all of our hits significantly increased the time required to recover half of the maximum fluorescence intensity (t_{half}), indicating less fluid lysosomal membrane in the hypodermis (Figure 2A-C, E, F). With some gene KDs, we also observed a decrease in the maximal recovered signal after bleaching (Figure 2D, G). The decrease in lysosomal membrane fluidity was not specific to the hypodermis as the KD of *spl-1* also increased the t_{half} of LAAT-1::mCherry in intestinal lysosomes (Figure S2A-D). To discern whether the detrimental effect of KD on membrane fluidity is confined to lysosomal membranes or extends to other cellular membranes, we utilized a *C. elegans* strain expressing a plasma membrane-anchored GFP[34]. Intriguingly, this reporter showed no change in the t_{half} with any KD and only *spl-1* KD led to decrease in the maximal recovered signal (Figure 2H-K, Figure S2E-G). Hence, the endolysosomal membrane seems to be particularly sensitive to a disruption of SL metabolism in contrast to the plasma membrane. Perturbing genes involved in both SL synthesis and degradation reduces the fluidity of the endolysosomal membrane and makes it more susceptible to rupture.

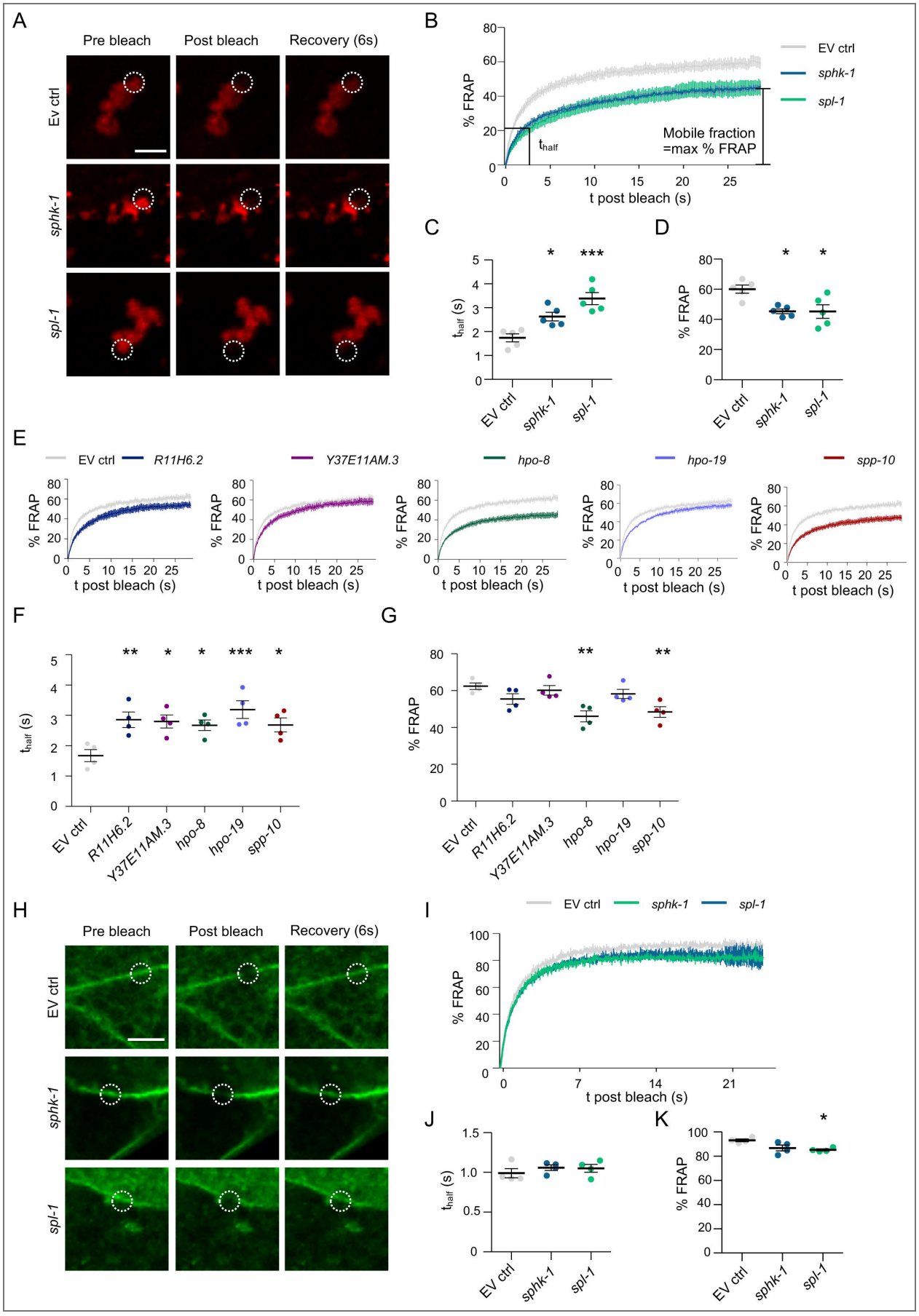
A
Pre bleach
Post bleach
Recovery (6s)
Ev ctrl
sphk-1
spl-1
B
% FRAP
t post bleach (s)
EV ctrl
sphk-1
spl-1
t half
Mobile fraction
=max % FRAP
C
t half (s)
D
% FRAP
E
EV ctrl
R11H6.2
Y37E11AM.3
hpo-8
hpo-19
spp-10
F
t half (s)
G
% FRAP
H
Pre bleach
Post bleach
Recovery (6s)
EV ctrl
sphk-1
spl-1
I
% FRAP
t post bleach (s)
J
t half (s)
K
% FRAP

Figure 2. Knockdown of genes involved in sphingolipid metabolism decreases lysosomal membrane fluidity.

(A) Representative confocal single plane images from a FRAP experiment in day 5 (second day of adulthood) animals expressing a mCherry tagged Lysosomal Lysine/Arginine Transporter 1 (LAAT-1::mCherry) in the hypodermis grown either on empty vector control (EV ctrl), *spl-1* or *sphk-1* RNAi plates. Dashed circles outline the bleach spots. Scale bar = 10 µm. **(B)** Combined FRAP curves of LAAT-1::mCherry in hypodermal lysosomal membranes. Curves are normalized to the pre-bleach intensity as 100% and the first post-bleach intensity as 0%. **(C, D)** Increase (C) in the mean time until half of the maximal signal is recovered (t_{half}) and decrease (D) in the maximal % recoverable fluorescence values upon KD of *sphk-1* and *spl-1* indicate a reduction in lysosomal membrane fluidity. **(E)** FRAP curves of LAAT-1::mCherry in hypodermal lysosomal membranes of animals grown either on empty vector or the indicated RNAi plates. Curves are normalized to the pre-bleach intensity set as 100% and the first post-bleach intensity as 0%. **(F)** Mean t_{half} upon KD of sphingolipid metabolism genes. **(G)** Maximal % recoverable fluorescence values upon KD of sphingolipid metabolism genes. **(H)** Representative confocal single plane images from a FRAP experiment in animals expressing prenylated GFP for lipid membrane anchorage in the intestine. Scale bar = 5 µm. **(I)** Combined FRAP curves of prenylated GFP enriched on the intestinal plasma membrane of animals grown either on empty vector, *sphk-1* or *spl-1* RNAi plates. Curves are normalized to the pre-bleach intensity as 100% and the first post-bleach intensity as 0%. **(J, K)** Mean t_{half} (J) and maximal % recoverable fluorescence values (K). Data represented as means ± SEM of 5 - 12 FRAP measurements per condition in animals on day 5 (second day of adulthood) collected in five biological replicates. Statistical analysis comparing RNAi conditions to the empty vector control was done using one-way ANOVA with Dunnett's post-hoc test. n.s.: not significant, * = p < 0.05, ** = p < 0.01, *** = p < 0.001.

KD of SPHK2 increases endolysosomal membrane rigidity in human cells

Having established in *C. elegans* that disruption of SL metabolism reduces endolysosomal membrane fluidity, we next asked whether this relationship is conserved in human cells. To this end, we employed SH-SY5Y human neuroblastoma cells and assessed membrane fluidity using C-Laurdan dye (Figure 3A). This approach leverages the unique properties of C-Laurdan, which emits fluorescent light of varying wavelengths in response to changes within the phospholipid bilayer, particularly reflective of membrane fluidity[35, 36]. The shift in emission profile between liquid-disordered and liquid-ordered phases allows a quantitative assessment of the membrane order by calculating the ratiometric relationship of the fluorescence intensity recorded in two spectral channels, known as a generalized polarization (GP) value[35] (Figure 3A). Decreasing GP values are indicative of increasingly fluid membrane while increasing GP values denote increased rigidity. Of note, we exposed the cells to C-Laurdan for an extended time of 2 hours (instead of 30 min as recommended in the original protocol), to promote internalization of the dye and thus increase the staining of endolysosomal membranes relative to the plasma membrane[35].

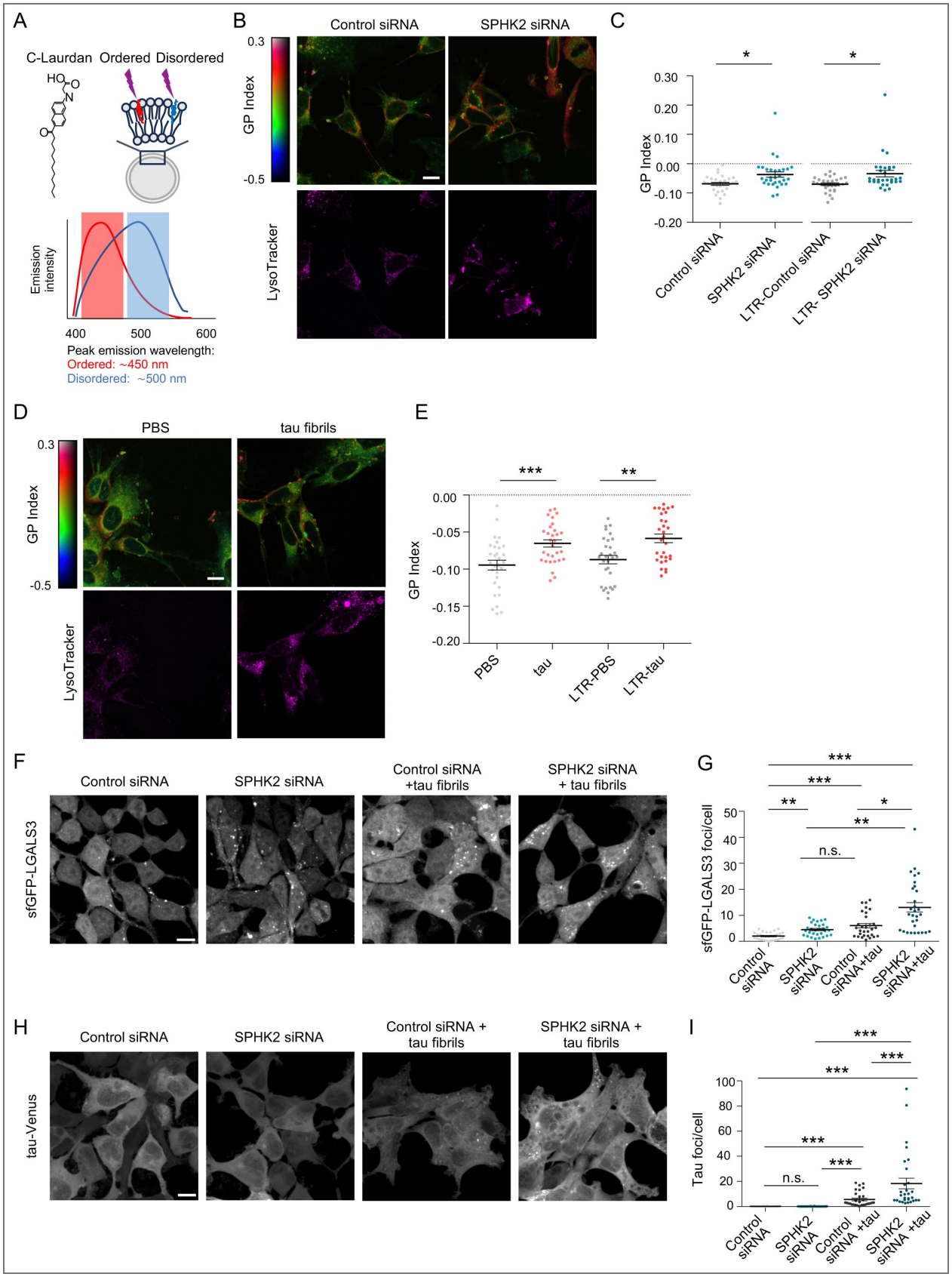

Figure 3. KD of SPHK2 and aggregated tau increases membrane rigidity leading to lysosomal rupture.

(A) Scheme of the fluorescence properties of C-Laurdan. The dye is excited at 405 nm and exhibits peak emission at 450 nm (red) in ordered membrane phases and ~500 nm in the disordered phase (blue). Two-channel acquisition is conducted in the wavelength bands indicated by shaded boxes. **(B)** Upper panels: Pseudo-colored images of SH-SY5Y cells transfected with control or SPHK2 siRNA showing the C-Laurdan GP Index at each pixel position. Lower panels show LysoTracker staining. Scale bar = 10 µm. **(C)** Quantification of GP values in SH-SY5Y cells upon transfected with control or SPHK2 siRNA. GP values were measured across the whole cell (left) or restricted to LysoTracker-positive (LTR) regions (right). Statistical analysis was conducted using a two-way mixed-model ANOVA, followed by pairwise comparisons of estimated marginal means with Sidak correction for multiple comparisons. n = 3 independent experiments, with 10 images analyzed per experiment. **(D)** Upper panel: Pseudo-colored images of SH-SY5Y cells exposed to PBS control or 1N4R tau fibrils showing the C-Laurdan GP Index at each pixel position. Lower panels show LysoTracker staining. Scale bar = 10 µm. **(E)** Quantification of GP values in SH-SY5Y cells exposed to PBS control or 1N4R tau fibrils. GP values were measured across the whole cell (left) or restricted to LysoTracker-positive (LTR) regions (right). Statistical analysis was conducted using a two-way mixed-model ANOVA followed by pairwise comparisons of estimated marginal means with Sidak correction for multiple comparisons. n = 3 independent experiments, with 10 images analyzed per experiment. **(F)** Maximum intensity projection of confocal z-stacks of HEK293T cells expressing sfGFP-LGALS3 upon treatment with control or SPHK2 siRNA, exposed to PBS control or 1N4R tau fibrils. Scale bar = 10 µm. **(G)** Quantification of sfGFP-LGALS3 foci per cell in HEK293T cells upon treatment with control or SPHK2 siRNA, exposed to PBS control or 1N4R tau fibrils. Data represent the mean number of foci per cell. Statistical analysis was done using Kruskal-Wallis with a Dunn's post-hoc test. N = 3 independent experiments, with 10 images analyzed per experiment. **(H)** Maximum intensity projection of confocal z-stacks of a P301S tau-Venus biosensor cell line upon treatment with control or SPHK2 siRNA with and without exposure to 1N4R tau fibrils. Scale bar = 10 µm. **(I)** Quantification of tau-Venus foci upon treatment with control or SPHK2 siRNA with and without exposure to 1N4R tau fibrils. Data were analyzed by a two-way mixed-model ANOVA, followed by pairwise comparisons were performed using estimated marginal means with Sidak correction. n = 3 independent experiments, with 10 images analyzed per experiment. n.s.: not significant, * = $p < 0.05$, ** = $p < 0.01$, *** = $p < 0.001$.

Upon KD of *SPHK2*, one of the human homologs of *C. elegans sphk-1*, the C-Laurdan fluorescence GP Index increased significantly, indicating increased membrane rigidity (Figure 3B, C). Lipofectamine treatment alone did not alter GP values (Figure S3A, B), and SPHK2 KD was confirmed by immunoblotting after 48 h and 72 h (Figure S3C–E). To determine whether SPHK2 KD affects lysosomal membrane fluidity, we combined C-Laurdan staining with LysoTracker staining and selectively analyzed LysoTracker-positive regions. SPHK2 KD resulted in a pronounced increase in GP values within LysoTracker-positive compartments, demonstrating increased membrane rigidity at lysosomes (Figure 3C). Taken together, FRAP and C-Laurdan analyses revealed that disruption of SL metabolism leads to more ordered and rigid endolysosomal membranes in both *C. elegans* and human cells.

Fibrillar tau and SPHK2 KD act in concert to exacerbate endolysosomal damage and seeded tau aggregation

Given that SPHK2 KD increased endolysosomal membrane rigidity and can compromise endolysosomal integrity, we next asked whether aggregated tau similarly alters membrane properties. Since fibrillar tau is known to induce endolysosomal rupture[14], we hypothesized that tau-induced membrane damage may also involve increased membrane rigidity. Treatment of SH-SY5Y and HEK293T cells with recombinant 1N4R tau fibrils led to a marked increase in membrane rigidity, as indicated by elevated GP values (Figure 3D, E, Figure S3F, G). This increase was also observed in LysoTracker-positive compartments, indicating increased rigidity of lysosomal membranes. Importantly, this effect was specific to fibrillar tau, as monomeric tau did not alter membrane fluidity (Figure S3H, I). These findings suggest that aggregated tau, like SPHK2 KD, promotes membrane rigidification, providing a potential mechanism by which tau fibrils may contribute to endolysosomal rupture.

We therefore asked whether SPHK2 KD further enhances tau-fibril-induced endolysosomal damage. To test this, we used a previously established HEK293T cell line stably expressing sfGFP-LGALS3 and monitored endolysosomal rupture by galectin puncta formation[20,29]. Cells were

treated with recombinant 1N4R tau fibrils, either alone or in combination with siRNA-mediated SPHK2 KD. Both, tau fibrils and SPHK2 KD alone induced endolysosomal rupture, as evidenced by increased sfGFP-LGALS3 puncta formation (Figure 3F, G and Figure S3J). While SPHK2 KD alone significantly increased galectin puncta above the matched control, its effect was more modest than in our previous CRISPR inhibition-based analysis[20]. This difference likely stems from the earlier readout required for the combined siRNA/tau fibril assay, when transient Lipofectamine-associated effects still increased the control background. Importantly, SPHK2 KD further enhanced tau fibril-induced sfGFP-LGALS3 foci formation, indicating that SL disruption compromises endolysosomal integrity and sensitizes endolysosomal membranes to tau fibril-induced damage in human cells.

Because endolysosomal rupture facilitates the escape of luminal contents, including tau seeds, into the cytosol, we next asked whether membrane perturbation by SPHK2 KD influences seeded tau aggregation. Using a HEK biosensor cell line expressing Venus-tagged full-length P301S mutant 0N4R tau (tau-Venus)[37, 38], we found that SPHK2 KD alone did not induce tau aggregation, as no increase in tau-Venus foci was observed (Figure 3H, I and Figure S3K). However, upon addition of recombinant tau fibrils, SPHK2 KD significantly increased tau-Venus foci formation. Thus, under the conditions tested here, disruption of SL metabolism alone is not sufficient to initiate detectable tau aggregation. Rather, it seems to facilitate the escape of tau seeds from the endolysosomal compartment into the cytosol by compromising endolysosomal membrane integrity.

Tau transmission sensitizes endolysosomal membranes to sphingolipid perturbations in vivo

To determine how tau transmission and SL perturbations interact to affect endolysosomal integrity in vivo, we returned to *C. elegans*. We compared animals expressing F3ΔK281::mCherry in touch receptor neurons, from where it is transmitted to the hypodermis, with matched controls expressing mCherry alone in the same neurons[20]. In both strains, sfGFP::LGALS3 is expressed in the hypodermis to monitor endolysosomal membrane damage[20]. KD of Y37E11AM.3 alone did not increase hypodermal sfGFP::LGALS3 puncta compared to EV control RNAi, whereas the presence of transmitted F3ΔK281::mCherry significantly increased galectin puncta (Figure 4A). In contrast, KD of the remaining SL-related hits resulted in nearly all animals displaying hypodermal sfGFP::LGALS3 foci in both genetic backgrounds. This suggests that strong disruption of SL metabolism is sufficient to overwhelm endolysosomal integrity independently of tau.

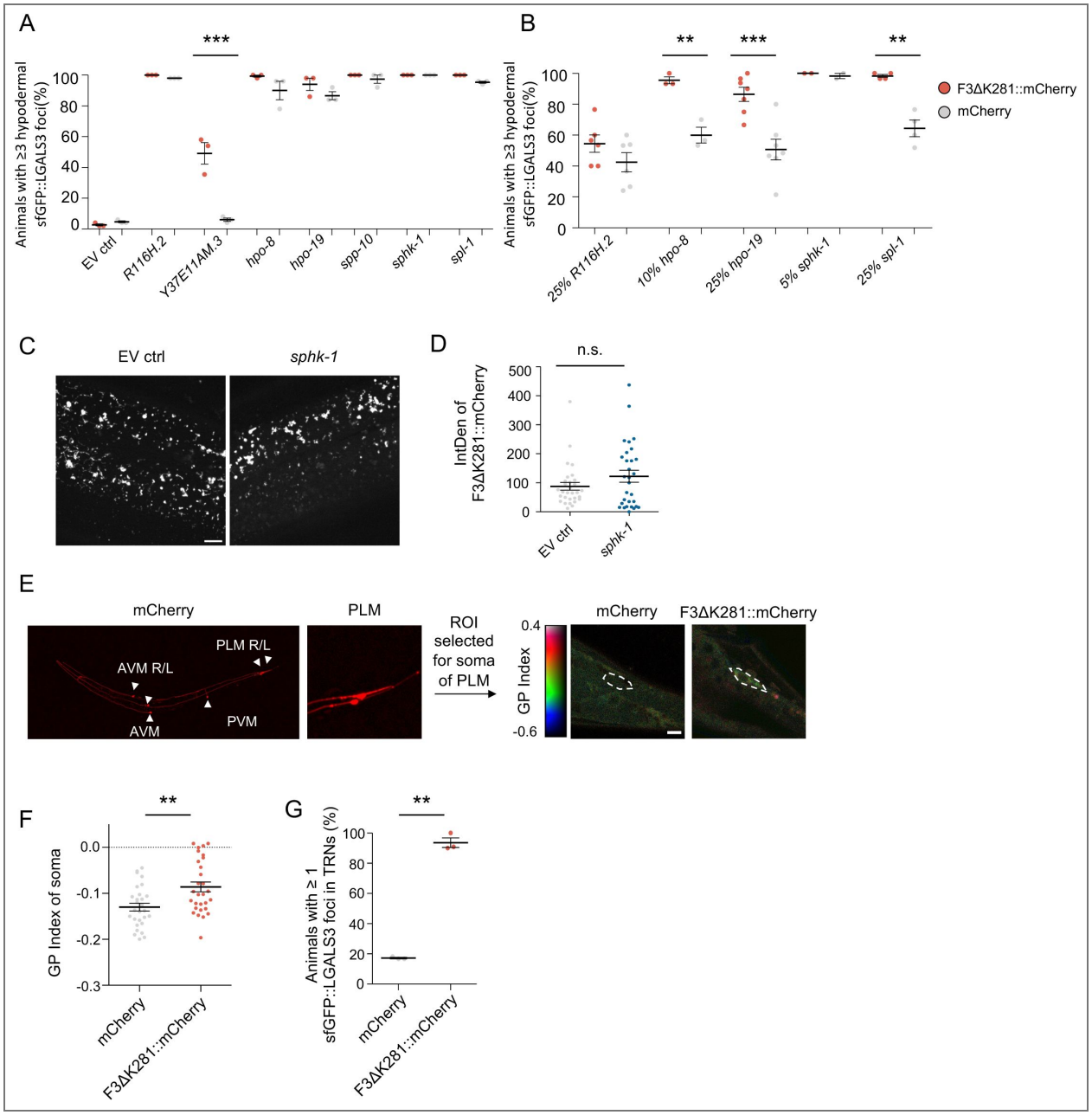

Figure 4. Aggregated tau promotes endolysosomal rupture.

(A, B) Quantification of the percentage of animals with ≥ 3 hypodermal sfGFP::LGALS3 foci, upon expression of either F3ΔK281::mCherry (red) or mCherry control (grey) in touch receptor neurons and KD of the indicated genes on day 5 (second day of adulthood) (A). Quantification of endolysosomal rupture under sub-saturating RNAi conditions. RNAi cultures were diluted with the empty vector (EV) control bacteria to reduce the KD strength (B). Data represented as mean ± SEM. n = 3 - 7 independent experiments with 40 - 50 (A) or 20 - 30 (B) animals analyzed per experiment. Since even a dilution down to 5% of the *sphk-1* RNAi resulted in 100% of animals being scored as positive in two independent replicates this condition was not repeated further. Statistical analysis comparing mCherry to F3ΔK281::mCherry under individual RNAi conditions was done using two-way ANOVA with Sidaks's post-hoc test. ** = $p < 0.01$, *** = $p < 0.001$. **(C)** Representative images of hypodermal F3ΔK281::mCherry signal in EV control or *sphk-1* RNAi treated animals on day 5 (second day of adulthood). Scale bar = 10 µm. **(D)** Quantification of hypodermal F3ΔK281::mCherry fluorescence intensity (integrated density, IntDen) in EV control or *sphk-1* RNAi treated animals on day 5 (second day of adulthood), indicating *sphk-1* KD does not alter tau transmission levels. Statistical analysis was done using Student's t-test. n = 3 independent experiments with 35 animals analyzed in total. **(E)** C-Laurdan staining

of animals expressing F3ΔK281::mCherry or mCherry in touch receptor neurons on day 4 (first day of adulthood). The mCherry signal was used to select a region of interest (ROI) around the soma of the posterior touch receptor neurons (PLM) to determine the GP value. Scale bar = 10 µm. **(F)** Quantification of GP values in animals expressing F3ΔK281::mCherry compared to mCherry on day 4 (first day of adulthood). Statistical analysis was done using a Student's t-test. n = 4 independent experiments, with at least 28 animals analyzed in total. **(G)** Quantification of the percentage of animals expressing mCherry or F3ΔK281::mCherry in touch receptor neurons with ≥1 sfGFP::LGALS3 puncta in touch receptor neurons on day 5 (second day of adulthood). Each dot represents an independent experiment, and lines indicate the mean ± SEM. n = 3 independent experiments, with 10-14 animals per experiment. Statistical analysis was done using a Student's t-test. n.s.: not significant, * = p < 0.05, ** = p < 0.01, *** = p < 0.001.

To determine whether tau-dependent effects were masked by the strength of RNAi, we titrated RNAi bacterial concentrations to achieve sub-saturating KD conditions. Under these conditions, KD of *spl-1*, *hpo-8*, and *hpo-19* induced endolysosomal damage that was significantly exacerbated in F3ΔK281::mCherry animals compared to mCherry controls (Figure 4B). In contrast, dilution of *R11H6.2* RNAi did not reveal tau-dependent differences, and *sphk-1* KD remained fully penetrant even at high dilution. Importantly, RNAi-mediated knockdown of *sphk-1* did not alter hypodermal F3ΔK281::mCherry levels, arguing that the enhanced rupture phenotype is not due to increased tau transmission (Figure 4C, D).

To assess whether tau directly alters membrane properties in vivo, we measured membrane fluidity in the somas of the posterior touch receptor (PLM) neurons using C-Laurdan dye. Expression of the tau fragment led to a decrease in membrane fluidity compared to mCherry controls (Figure 4E, F), indicating that tau promotes membrane rigidification in PLM neurons, consistent with our observations in human cells (Figure 3D, E). In addition, expression of sfGFP-LGALS3 in touch receptor neurons revealed increased galectin puncta in animals expressing F3ΔK281::mCherry compared to mCherry controls, indicating elevated endolysosomal rupture in neurons (Figure 4G). These findings suggest that perturbation of SL metabolism and tau accumulation both increase endolysosomal membrane rigidity and make vesicles more prone to rupture, with additive effects when both perturbations occur simultaneously.

Increasing membrane fluidity reduces aggregated tau-mediated endolysosomal damage, seeded aggregation, and neurotoxicity

SL metabolism can influence cellular physiology through multiple mechanisms beyond its effects on membrane fluidity. To test more directly whether altered membrane fluidity contributes to aggregated tau-induced endolysosomal damage and propagation, we used fatty acid supplementation as an independent approach to modulate lipid packing. Saturated fatty acids such as palmitic acid (PA) promote tight lipid packing and increase membrane rigidity, whereas unsaturated fatty acids contain one or more double bonds that introduce kinks into their hydrocarbon chains, resulting in looser lipid packing and increased membrane fluidity.

We first increased membrane rigidity with PA. PA treatment increased membrane rigidity in SH-SY5Y and HEK293T cells (Figure S4A–F), exacerbated tau fibril-induced sfGFP-LGALS3 foci formation (Figure S4G,H), and enhanced tau-Venus aggregation after exposure to tau fibrils (Figure S4I,J). These findings support a model in which increased membrane rigidity promotes endolysosomal damage and facilitates tau propagation.

We next asked whether increasing membrane fluidity could counteract these effects. Treatment of SH-SY5Y and HEK293T cells with the ω-3 polyunsaturated fatty acid (PUFA) α-linolenic acid (ALA) increased membrane fluidity (Figure S5A-C) and prevented tau fibril-induced membrane rigidification (Figure 5A, B and Figure S5D). Consistent with this, LysoTracker-based analysis indicated that ALA also affected lysosome-associated membrane properties. Moreover, ALA pre-treatment reduced tau fibril-induced endolysosomal rupture (Figure 5C, D and Figure S5E).

Since ALA prevented endolysosomal rupture, we expected it to also prevent seeded tau aggregation. Indeed, tau-Venus cells pre-loaded with ALA exhibited significantly fewer foci when exposed to tau fibrils (Figure 5E, F and Figure S5F). Together, these data show that increasing

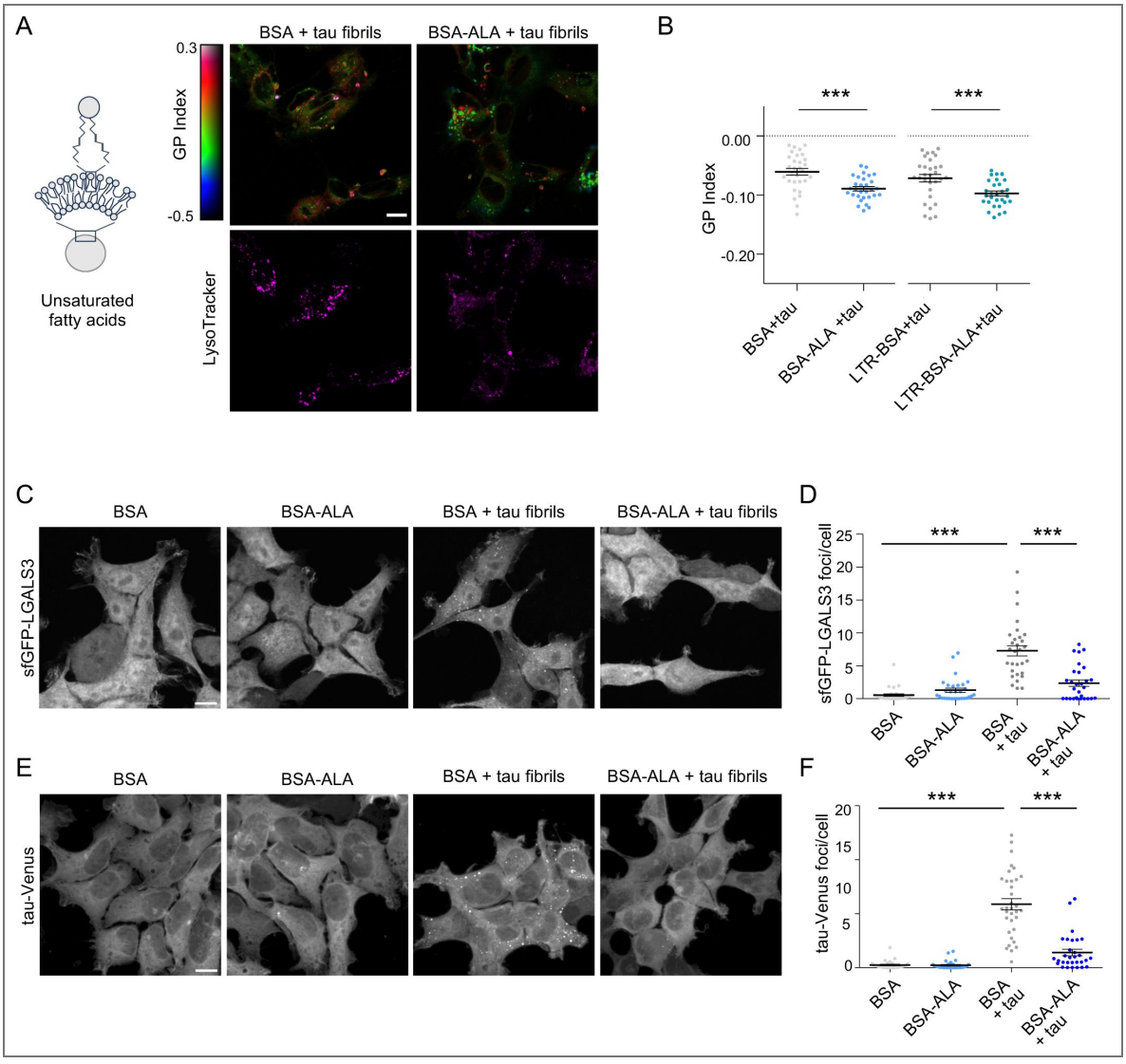

Figure 5. PUFA supplementation restores lysosomal membrane integrity and reduces seeded tau aggregation.

(A) Left: unsaturated fatty acid membrane scheme. Right: Pseudo-colored images of SH-SY5Y cells pre-loaded with BSA control or 150 µM ALA conjugated to BSA (BSA-ALA) and treated with 1N4R tau fibrils showing the C-Laurdan GP Index at each pixel position. Lower panels show LysoTracker staining. Scale bar = 10 µm. **(B)** Quantification of GP values in SH-SY5Y cells pre-loaded with BSA control or 150 µM ALA conjugated to BSA (BSA-ALA) and exposed to 1N4R tau fibrils. GP values were measured across the whole cell (left) or restricted to LysoTracker-positive (LTR) regions (right). Statistical analysis was conducted using a two-way mixed-model ANOVA, followed by pairwise comparisons of estimated marginal means with Sidak correction for multiple comparisons. n= 3 independent experiments, with 10 images analyzed per experiment. **(C)** Maximum intensity projection of confocal z-stacks of HEK293T cells expressing sfGFP-LGALS3 pre-loaded with BSA or BSA-ALA with or without exposure to 1N4R tau fibrils. Scale bar = 10 µm. **(D)** Quantification of sfGFP-LGALS3 foci following indicated treatments. Statistical analysis comparing BSA + tau to other conditions was done using Kruskal-Wallis with Dunn's post-hoc test. n = 3 independent experiments, with 10 images analyzed per experiment. *** = $p < 0.001$. **(E)** Maximum intensity projection of confocal z-stacks of tau-Venus biosensor cell line pre-loaded with BSA or BSA-ALA with or without exposure to 1N4R tau fibrils. Scale bar = 10 µm. **(F)** Quantification of tau-Venus foci following indicated treatments. Statistical analysis comparing BSA + tau to other conditions was done using Kruskal-Wallis with Dunn's post-hoc test. n = 3 independent experiments, with 10 images analyzed per experiment. *** = $p < 0.001$.

lysosomal membrane fluidity counteracts tau fibril-induced endolysosomal membrane damage and limits downstream seeded tau aggregation.

Finally, we asked whether ALA would also reduce the toxicity associated with aggregated tau in our *C. elegans* model. Expression of F3ΔK281::mCherry in touch receptor neurons resulted in an age-dependent decline in the response to gentle touch from day 4 (first day of adulthood) to day 8 (day 5 of adulthood) (Figure 6A, and Figure S6)[20]. Supplementation of ALA significantly mitigated this behavioral deficit (Figure 6A and Figure S6) and reduced neurotoxicity (Figure 6B, C). Consistent with improved neuronal integrity, ALA treatment also reduced sfGFP::LGALS3 foci in touch receptor neurons (Figure 6D), indicating decreased endolysosomal damage in vivo. Together, these findings show that ALA-mediated increase in membrane fluidity reduces tau fibril-induced lysosomal membrane rigidification, endolysosomal damage, and seeded tau aggregation in human cells, while attenuating tau-associated neuronal dysfunction and endolysosomal damage in *C. elegans*.

Discussion

Building on our previously published genome-wide screen in *C. elegans*, which identified SL metabolism as a regulator of endolysosomal integrity[20], we investigated how genetic perturbation of enzymes involved in SL metabolism promotes endolysosomal membrane rupture and tau-associated phenotypes. We found that disruption of SL metabolism decreases endolysosomal membrane fluidity, making vesicles more prone to rupture. Fibrillar tau had a similar effect on membrane rigidity and acted additively with perturbation of SL metabolism to exacerbate endolysosomal damage. In human cell models, disruption of SL metabolism enhanced tau-fibril-induced rupture and seeded tau aggregation, whereas increasing membrane fluidity with ALA reduced tau-induced membrane rigidification, endolysosomal damage, and seeded aggregation. In *C. elegans*, ALA attenuated aggregated tau-associated neuronal dysfunction and endolysosomal damage. Together, these findings support a model in which disruption of SL metabolism and tau accumulation converge on endolysosomal membrane rigidification, thereby promoting endomembrane rupture, and allowing tau seeds to escape into the cytosol, where they seed the aggregation of soluble endogenously expressed tau.

Our results show that reducing the expression of genes involved in both, biosynthesis and degradation of SLs significantly reduced the fluidity of endolysosomal membranes, making them more fragile and prone to rupture. KD of the saposin *spp-10*, the sphingosine kinase *sphk-1*, and the sphingosine-1-phosphate lyase *spl-1* blocks the degradation of complex SLs and should lead to an increase in their relative abundance, and therefore to a decrease in membrane fluidity. KD of the very-long-chain (3R)-3-hydroxyacyl-CoA dehydratase *hpo-8*, which is involved in fatty acid elongation, has been demonstrated to promote the incorporation of long-chain UFAs into phospholipids, thereby restoring plasma membrane fluidity[39]. The absence of *hpo-8* leads to membrane rigidification[39]. Conversely, KD of the serine incorporator *R11H6.2* and the 3-ketodihydrosphingosine reductase *Y37E11AM.3*, which function in the SL de novo synthesis pathway, should theoretically decrease total SL content and consequently increase membrane fluidity. The cytochrome b5 reductases *hpo-19* and *T05H4.4*, required for lipid desaturation, are involved in the conversion of dihydroceramide to ceramide and the biosynthesis of PUFAs[40]; KD of these genes is expected to reduce the levels of SLs and PUFAs, which could theoretically either increase or decrease membrane fluidity, depending on which metabolic pathway is predominantly affected.

Our observation that KD of all these genes results in decreased membrane fluidity is therefore seemingly counterintuitive. However, SLs form a complex metabolic network and can interconvert, allowing dynamic adaptation of SL levels. In addition, cells may compensate for the loss of certain SLs by altering the biosynthesis or turnover of other lipid molecules. This dynamic interplay makes it difficult to predict how individual gene knockdowns affect endolysosomal membrane composition and biophysical properties. Thus, genes that act at apparently opposing steps of SL metabolism could still converge on similar changes in membrane packing and fluidity. Lipidomic analyses will be important to determine how SL perturbations remodel cellular and

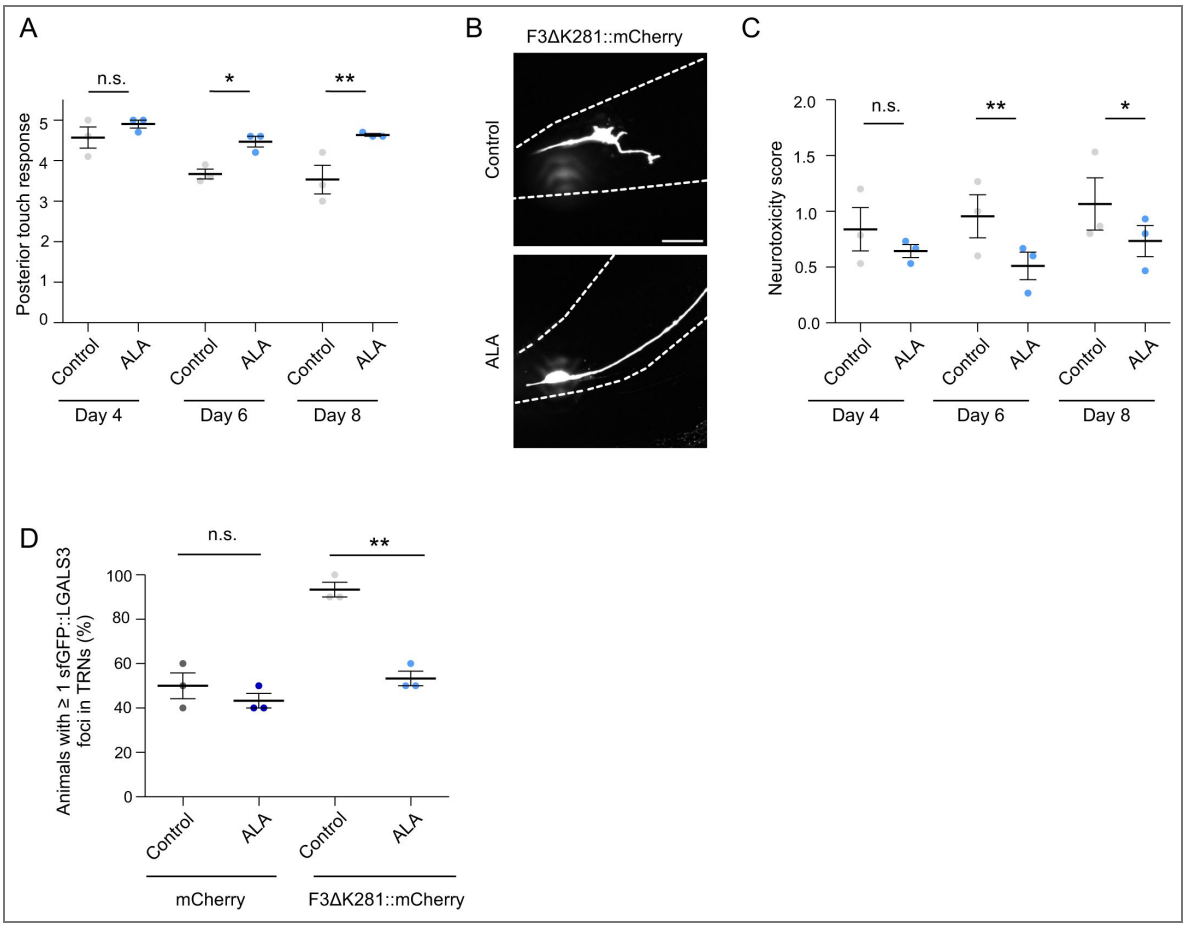

Figure 6. ALA improves neuronal function and reduces toxicity during aging.

(A) Posterior touch response of animals expressing F3ΔK281::mCherry at indicated ages when grown on plates supplemented with ALA or ethanol solvent only control. Statistical analysis was done using two-way ANOVA with Bonferroni's multiple comparison test. n = 3 independent experiments, with 10 animals analyzed per experiment. **(B)** Maximum intensity projection of confocal z-stacks of day 6 old animals expressing F3ΔK281::mCherry grown on EtOH solvent control or ALA plates. Scale bar = 20 µm. **(C)** Neurotoxicity score of PLM neurons of animals expressing F3ΔK281::mCherry grown on EtOH solvent control or ALA plates at indicated ages. Statistical analysis was done using two-way ANOVA with a Holm-Sidak's multiple comparison test. n = 3 independent experiments, with 15 animals analyzed per experiment. **(D)** Quantification of the percentage of animals with ≥1 sfGFP::LGALS3 puncta in touch receptor neurons, upon co-expression of either mCherry control or F3ΔK281::mCherry and growth on EtOH solvent control or ALA-supplemented plates on day 5 (second day of adulthood). Statistical analysis was done using two-way ANOVA with Bonferroni's multiple comparison test. Each dot represents an independent experiment, lines indicate the mean ± SEM. n= 3 independent experiments, with 10 animals analyzed per experiment. n.s.: not significant, * = $p < 0.05$, ** = $p < 0.01$.

organellar lipid composition. However, even detailed lipidomics would not by itself identify which lipid changes are responsible for the observed membrane rigidification. Indeed, membrane fluidity is not determined by a single lipid species, but by the combined properties of the entire membrane, including lipid abundance, saturation, acyl-chain length, head groups, sterol content, and membrane-associated proteins. Thus, an increase or decrease in a given lipid species cannot be directly translated into a predictable change in membrane fluidity without additional functional validation. Future lysosome-enriched or organelle-specific lipidomic approaches, ideally complemented by analyses of membrane-associated proteins, will therefore need to be combined with direct manipulation of candidate lipid or protein species, followed by measurements of membrane fluidity and rupture, to determine which molecular changes causally contribute to endolysosomal membrane rigidification.

Importantly, endolysosomal membrane rupture and global lysosomal function are related but not identical readouts. This distinction is supported by work showing that lipid dysregulation can induce lysosomal membrane permeabilization and lysosomal accumulation of endogenous protein aggregates without broadly impairing core lysosomal or proteasomal functions[41]. Thus, membrane damage can occur even when general lysosomal activity is not overtly disrupted. Conversely, a recent study independently identified SPHK-1 as an important regulator of lysosomal integrity in *C. elegans*, showing that strong *sphk-1* loss-of-function causes lysosomal sphingosine accumulation, membrane rupture, impaired degradative function, cargo accumulation, developmental defects, and reduced lifespan[42]. Together, these studies suggest that the functional consequences of disrupted SL metabolism can vary depending on allele strength, tissue, developmental stage, and assay conditions. In the present study, we focused on endolysosomal membrane fluidity and rupture because these membrane-level changes are directly linked to tau seed escape and seeded aggregation.

The central nervous system (CNS) is particularly rich in lipids. Approximately 50% of the brain's dry weight consists of lipids with high concentrations of cholesterol, phospholipids and sphingolipids[43, 44]. Alterations in lipid and SL metabolism have been observed not only during the aging process, but also in various late-onset neurodegenerative diseases including AD[26, 45]. While aging is the major risk factor for AD, one of the most significant genetic risk factors for AD is the apolipoprotein E (ApoE) polymorphism, specifically the ApoE4 allele[46]. ApoE is the primary lipoprotein in the brain, crucial for lipid transport and metabolism. Besides cholesterol, the ApoE4 variant has been shown to influence SL metabolism, thereby affecting the pathogenesis of AD from its early stages[26, 45, 47]. Thus, although disturbances in SL homeostasis are increasingly recognized in AD, the mechanisms by which they contribute to disease progression remain poorly understood.

AD brains exhibit elevated levels of sphingosine, ceramide 1-phosphate, and ceramide compared to control subjects[45]. Multivariate analysis and machine learning also identified these SL species as key contributors to AD[45]. However, these analyses were performed in different brain regions without cell-type or subcellular resolution. We found that perturbation of SL metabolism primarily affected endolysosomal membranes, with little effect on plasma membrane fluidity in *C. elegans*. In human cells, LysoTracker-based analysis further revealed pronounced increases in GP values within lysosome-associated compartments. The lysosomal membrane is particularly rich in sphingolipids[48], which may make it especially sensitive to perturbation of SL metabolism. Studies in yeast have shown that increased membrane lipid saturation affects the vacuole—the functional counterpart of mammalian lysosomes—as well as the nuclear envelope, whereas the plasma membrane and mitochondria remained relatively unaffected[49]. These findings indicate that cellular membranes vary in their resilience to lipid saturation stress, potentially due to differences in lipid composition and protective mechanisms[49, 50]. To better understand the implications of SL alterations in AD, it would be important to examine whether the observed changes primarily originate from endolysosomal membranes or also from other organelles, such as the endoplasmic reticulum and the nucleus, or from the plasma membrane.

We observed that fibrillar tau also increased membrane rigidity and exacerbated endolysosomal rupture. This suggests that tau accumulation and disruption of SL metabolism may converge on a common biophysical mechanism. This interpretation is consistent with recent ultrastructural studies showing that intralysosomal amyloid assemblies can physically deform and rupture lysosomal membranes[51, 52]. Whether this mechanism is specific to tau or also applies to other amyloid assemblies remains to be determined. In *C. elegans*, tau transmission sensitized endolysosomal membranes to SL perturbation, especially under sub-saturating RNAi conditions. The enhanced rupture phenotype is unlikely to result from a direct effect of RNAi on neuronal F3ΔK281::mCherry expression, as *C. elegans* neurons are largely refractory to systemic RNAi under the conditions used here[53]. Consistent with this, *sphk-1* RNAi did not alter hypodermal F3ΔK281::mCherry levels, supporting the interpretation that SL perturbation increases endolysosomal membrane damage rather than tau transmission itself.

These findings also raise the possibility that alterations in SL metabolism are not only a cause but also a consequence of tau-associated pathology[26, 45]. Accumulation of misfolded tau in lysosomes could impair lysosomal clearance capacity and alter lipid turnover, leading to accumulation of membrane lipids or other biomolecules. In turn, impaired SL metabolism could further reduce endolysosomal membrane fluidity and promote rupture. Such a cycle, in which imbalances in proteostasis and lipostasis negatively influence each other, may contribute to progressive lysosomal dysfunction and neurodegeneration[54].

Manipulating membrane fluidity independently of SL enzymes further supported a role for membrane biophysics in tau-induced endolysosomal damage. Increasing membrane rigidity with PA exacerbated tau-induced rupture and seeded aggregation, whereas increasing membrane fluidity with ALA reduced tau-induced lysosomal membrane rigidification, endolysosomal damage, and seeded aggregation in cells and attenuated tau-associated neuronal dysfunction in *C. elegans*.

Given the high levels of saturated and trans fats in the Western diet[55], it is plausible that dietary factors contribute to the dysregulation of lipid homeostasis in the brain. In line with a broader role of lipid saturation in AD, a recent plasma lipidomics study reported reduced highly unsaturated lipid species and increased saturated lipid species in women with AD[56]. The Mediterranean UFA-rich diet has been associated with healthy aging, while reduced UFA brain levels have been correlated with increased tau and Aβ pathology and decreased cognitive function in AD[57, 58]. Our findings therefore provide a possible mechanistic explanation for the beneficial effects of PUFA-rich diets or PUFA supplementation reported in AD-related contexts[59, 60]. However, PUFAs can also influence lipid signaling, oxidative stress responses, and broader membrane remodeling. We therefore cannot exclude additional direct or indirect effects of ALA. Nevertheless, the opposing effects of PA and ALA, together with the SL knockdown data, support the interpretation that membrane fluidity is a major determinant of endolysosomal membrane integrity and rupture in our models.

In sum, our study identifies endolysosomal membrane fluidity as a key determinant of vesicle integrity in the context of disrupted SL metabolism and tau accumulation. We propose that perturbation of SL metabolism and fibrillar tau converge on membrane rigidification, thereby reducing endolysosomal membrane integrity and promoting vesicle rupture, tau seed escape, and seeded tau aggregation. Restoring membrane fluidity may therefore represent a strategy to limit tau-induced endolysosomal damage and tau-associated toxicity, although the lipid species, membrane compartments, and additional cellular pathways contributing to this protection remain to be defined.

Methods

Maintenance of *C. elegans*, RNAi experiments and age synchronization

All animals were cultured using standard methods[61]. If not otherwise indicated, worms were grown on nematode growth medium (NGM) plates seeded with *E. coli* strain OP50 at 20 °C. For RNAi, NGM medium was supplemented with Ampicillin, Tetracycline, and IPTG, seeded with the respective HT115 *E. coli* RNAi clones (from the Ahringer RNAi library, for details see Table S2) and grown at 20 °C. For diluted RNAi experiments, RNAi was diluted with EV control bacteria. Animals were age-synchronized by bleaching. Briefly, gravid adults were dissolved in 20% sodium hypochlorite solution. The surviving *C. elegans* embryos were hatched overnight in M9 buffer with gentle rocking at 20 °C. The next day, appropriate amounts of L1 larvae were added to the plates.

Cloning and generation of the neuronal sfGFP::LGALS3 strain

The sfGFP::LGALS3 reporter sequence was amplified from a previously cloned plasmid[20] via PCR using suitable primers for subsequent Gibson assembly. The pCFJ150 vector backbone already containing an rgef-1p::GFP1-10::tbb2-3'UTR construct was cut via restriction digestion using NheI (NEB #R0131) and BglII (NEB #R0144) to remove the GFP1-10 sequence. The sfGFP::LGALS3 construct was subsequently cloned into this vector backbone in a Gibson assembly reaction using 0.08 pmol of plasmid backbone and a 5-fold molar excess of insert. 10 µl of fragment-vector mix was added to 10 µl Gibson assembly reaction mix containing 1.3x ISO buffer (6.5% w:v PEG-8000 [Sigma-Aldrich 89510], 130 mM Tris-HCl (Carl Roth, 4855.2) pH = 7.5, 13 mM MgCl2 (Carl Roth, A537.1), 13 mM DTT (Sigma-Aldrich 43816), 0.26 mM each dATP, dTTP, dCTP, and dGTP (NEB, N0446), 1.3 mM NAD (NEB, B9007S)), 0.05 U T5 exonuclease [NEB, M0663], 0.3 U Phusion polymerase (Thermo Fisher Scientific, F530), and 50 U Taq ligase [NEB, M0208L] and incubated at 50 °C for 2h. Subsequently the whole reaction was used to transform chemically competent *E. coli*. The extrachromosomal array was created by microinjecting the expression plasmid rgef-1p::sfGFP::LGALS3::tbb2-3'UTR (30 ng/µl) into the gonads of young adult wildtype *C. elegans* (N2s), together with a co-injection marker (15 ng/µl) for expression of RFP in coelomocytes. All strains generated or used in this study are found in Table S1.

C. elegans fatty acid supplementation

Polyunsaturated fatty acids were dissolved in EtOH and stored in the dark at -20 °C under a N_2 atmosphere to prevent oxidation. NGM was cooled after autoclaving to 55 °C. To enhance fatty acid distribution, NP-40 substitute (0.001% v/v) was added to the media and subsequently either 0.3 mM of the desired fatty acid solution or the ethanol solvent as control and stirred for 5 min before plate pouring[62]. Palmitic acid (PA) was supplemented by enriching the OP50 bacterial food source[63]. Overnight cultures were grown in the presence of 2 mM of PA dissolved in EtOH or EtOH alone. The next day, OP50 bacteria were pelleted by centrifugation (10 min at 4500x g) and washed 2x with M9 buffer[64]. 10x concentrated bacteria (in M9) were then seeded on NGM plates.

Quantification of lysosomal rupture (galectin puncta assay) in *C. elegans*

Quantification of animals showing hypodermal lysosomal rupture was done as previously described[29, 65]. Briefly, age-synchronized animals expressing the sfGFP::LGALS3 construct in the hypodermis were seeded on OP50 or RNAi NGM plates. Scoring was done on day 5 (second day of adulthood) using a Leica M205 FA widefield binocular microscope. 20-50 worms were analyzed per replicate. *Sphk-1* mutant animals were obtained from CGC (CZ24969; *sphk-1(ju831)*) and crossed with animals expressing sfGFP::LGALS3 in the hypodermis.

Formation of sfGFP::LGALS3 foci in touch receptor neurons was quantified in day 5 (second day of adulthood) old animals co-expressing either mCherry or F3ΔK281::mCherry in touch receptor neurons using an Olympus IXplore SpinSR confocal microscope equipped with a UPlanSApo

60×/1.30 silicone oil objective. Foci formation was checked using a 488 nm laser at 80% power with an exposure time of 200 ms. An animal was counted as positive for endolysosomal rupture if it had at least one sfGFP:: LGALS3 foci in the PLM or ALM neurons.

Mounting of live animals for imaging

Synchronized animals were mounted on 8-10% agarose in M9 buffer pads with a drop of mounting mix (2% (w/v) levamisole and 50% (v/v) nanosphere size standards (Thermo Fisher)) and covered with a coverslip.

Fluorescence recovery after photobleaching (FRAP)

FRAP measurements to estimate membrane fluidity were done following a published protocol[66]. Animals were synchronized by bleaching and grown until day 5 (second day of adulthood) on the indicated RNAi or empty vector (EV) control plates. Directly before the FRAP experiments, animals were mounted at the Zeiss LSM 780 confocal microscope. FRAP measurements of either GFP enriched in the intestinal plasma membrane, or LAAT-1::mCherry located in intestinal or hypodermal lysosomal membranes were taken with 40X Water immersion objective. For the lysosomal membrane, mCherry-positive membranes were photobleached over a circular area (seven pixel radius) using 10 iterations of the 561 nm DPSS laser with 100% laser power transmission. Images were collected at a 12-bit intensity resolution over 128 × 128 pixels (digital zoom 6X) using a pixel dwell time of 3.15 µsec with 2% laser power transmission. For the plasma membrane, GFP-positive membranes were photobleached over a circular area (10 pixel radius) using 20 iterations of the 488 nm Argon laser with 100% laser power transmission. Images were collected at a 12-bit intensity resolution over 128 × 128 pixels (digital zoom 6X) using a pixel dwell time of 3.15 µsec with 10% laser power transmission. At least 6 pre-bleaching images were collected before the region of interest was bleached. The recovery of fluorescence was traced for 25s. Fluorescence recovery and T_{half} were calculated as previously described in Svensk et al.[67].

Quantification of spreading

Transmission of F3ΔK281::mCherry was quantified as previously published in Sandhof et al.[20]. In short, the hypodermis of age-synchronized worms expressing F3ΔK281::mCherry in touch receptor neurons were imaged on day 5 (second day of adulthood) using an Olympus IXplore SpinSR confocal microscope equipped with a UPlanSApo 60×/1.30 silicone oil objective. Images were acquired using a 561 nm laser at 30% power with an exposure time of 450 ms. Z-stacks were collected at 0.35 µm intervals, and hypodermal fluorescence intensity (integrated density) was quantified using ImageJ.

Touch sensory assay and neurotoxicity in touch receptor neurons

Touch sensory assay was done as previously described[68]. Briefly, touch sensitivity was tested by gently stroking the tip of an eyebrow hair attached to a toothpick transversely across the anterior or posterior half of an animal. A touch-sensitive animal was one that stopped/moved away from the stimulus. 10 worms were examined for each strain in 3 biological replicates with 5 strokes in the anterior and posterior. For neurotoxicity scoring of the PLM neurons, live animals were imaged using an Olympus IXplore SpinSR Confocal microscope with an UplanS Apo 60x/1.30 Silicon oil objective. The neurotoxicity score was determined by adding a score of 1 for each of the following phenotypes: soma outgrowth, process branching, process break, wavy process. 15 animals were examined at each day of age in 3 independent biological replicates.

Cell culture

SH-SY5Y and HEK293T cells were cultured in DMEM containing high glucose, GlutaMAX Supplement, pyruvate (Gibco), and 10% FBS (Gibco) at 37 °C and 5% CO_2. Regular mycoplasma tests were performed (GATC Biotech). HEK293T cells expressing Venus-tagged full-length P301S mutant 0N4R tau (0N4R tauP301S-Venus) were kindly provided by Dr. William A. McEwan, Cambridge University[37].

Quantification of lysosomal rupture (galectin puncta assay) and tau-Venus foci in cells

Cells were imaged on an Olympus IXplore SpinSR Confocal microscope with an UplanS Apo 60x/1.30 Silicon oil objective. To detect the number of foci in an image, a difference of gaussian blur was applied to maximum projections to isolate foci from cytosolic sfGFP or Venus signal, respectively. Thresholding was applied using 'moments' threshold on FIJI. Number of foci was counted using the 'analyze particles' function. Cell number was counted manually to obtain number of foci/cell for each image.

C-Laurdan dye measurement of membrane fluidity in worms and cells

Live worms were stained with 10 mM C-Laurdan dye (6-dodecanoyl-2-dimethylaminonaphthalene) (Thermo Fisher Scientific) as previously described[69]. ROI was drawn around the soma of the PLM using the mCherry signal and only the GP values in this ROI were collected. Cells were also stained with C-Laurdan at 15 µM for 2 hours in combination with LysoTracker (Thermo Fisher Scientific) at 50 nM, cells were then fixed in 4% PFA in PBS. Images were acquired with an DMI6000 confocal microscope and Leica software with a 63x oil-immersion objective, with a zoom factor of 4 or with a Leica SP8X WLL microscope, equipped with 405 nm laser, WLL2 laser (470 - 670 nm) and acusto-optical beam splitter. Images were acquired with a 63×1.4 objective. Samples were excited with a 405 nm laser and the emission recorded between 400 and 460 nm (ordered phase) and between 470 and 530 nm (disordered phase). Quantitative assessment of the membrane order was achieved by calculating the ratiometric relationship of the fluorescence intensity recorded in two spectral channels (GP value) by using an automated ImageJ macro, according to published guidelines[35]. LysoTracker-positive regions were identified by thresholding the LysoTracker channel, and GP values were extracted from these regions using the macro cited above.

Knockdown of target genes by RNAi in cells

SPHK2 or a scrambled control siRNA were purchased from Thermo Scientific Dharmacon (ONTarget plus siRNA and Control Pool). Cells were seeded in DMEM with 10% FBS. siRNA was diluted in siRNA buffer (Final concentration 20 nM) before mixing with Lipofectamine 2000 for 20 min prior to being added to cells. To minimize Lipofectamine impact on the endolysosomal system, media was exchanged after 6 hours.

SDS-PAGE and immunoblotting

Cells were pelleted by centrifugation followed by lysis in lysis buffer (10mM Tris, 100mM NaCl, 0.2% Triton X-100, 10mM EDTA) on ice for 20 min. The lysates were transferred into fresh Eppendorf tubes and centrifuged (1000 g for 1 min at 4 °C) in a tabletop centrifuge to remove cellular debris. The protein concentration was determined using protein assay dye reagent concentrate (Bio-Rad). Proteins were separated under denaturing conditions by SDS–PAGE and transferred onto a PVDF membrane (Carl Roth) by standard wet blotting protocols. Samples were probed with rabbit polyclonal anti-SPHK2 (1:5000, 9C5E1, Santa Cruz) primary antibody. Mouse monoclonal anti-GAPDH antibody (1:5000, clone GAPDH-71.1, Sigma-Aldrich) was used as loading control. HRP-conjugated anti-mouse and anti-rabbit IgG secondary antibodies (Bio-Rad) were used for subsequent ECL-based detection (Bio-Rad).

Fatty acid treatment in cells

For α-linolenic acid (ALA), a stock solution was made in EtOH and stored in the dark at -20°C under a N_2 atmosphere to prevent oxidation[70]. Palmitic acid (PA) was dissolved in 0.1 M NaOH according to Cousin et al.[71]. ALA and PA were then conjugated to BSA in 10% fatty acid free solution by shaking for 1 hour at 37°C to a concentration of 6 mM for ALA and 5 mM for PA[72]. Prior to preloading cells with BSA-PA, the solution was heated to 65 °C for 15 min. For assays with C-Laurdan, cells were preloaded with FAs for 3 hours before the addition of C-Laurdan for another 2

hours. If preloading was followed by seeding with tau, preloading with FAs was done for 3 hours before fibrillar tau was added for an additional 5 hours. C-Laurdan was spiked in for the last 2 hours. No media changes were done between steps. For experiments with HEK293T tau-Venus cells and HEK293T sfGFP-LGALS3 cells, preloading with FAs was done for 3 hours before seeding with 1N4R tau fibrils. Cells were then fixed after 48 hours.

Monomeric and fibrillar tau

Full-length human 1N4R tau was expressed and purified as previously described[73]. The purified monomeric tau was dialyzed against PBS buffer containing 1 mM DTT, flash frozen in liquid nitrogen and stored at -80 °C. The concentration of monomeric tau was determined spectrophotometrically using an extinction coefficient at 280 nm of 7575 M^{-1} cm^{-1}. Monomeric 1N4R tau was assembled into fibrils at 40 µM in the presence of 10 µM heparin, in PBS buffer containing 1 mM DTT under continuous shaking (600 rpm) for 5 days at 37 °C in an Eppendorf Thermomixer. The quality of 1N4R tau fibrils produced after 5 days was assessed by ThioflavinT binding, sedimentation, and transmission electron microscopy (TEM). The resulting 1N4R tau fibrils were spun at 25 °C and 75 000 g for 30 min. The pelleted fibrils were resuspended in PBS buffer with 1 mM DTT at 50 µM equivalent monomeric tau concentration. 1N4R tau fibrils were labeled by incubation with the 2 molar equivalents of lysine-reactive ATTO 550 (ATTO-TEC, GMBH) for 1 h at room temperature. The unreacted fluorophore was removed by two cycles of centrifugation at 75 000 g for 10 min and resuspension of the pellet in PBS. 1N4R tau fibrils were fragmented by sonication for 5 min in 2-ml Eppendorf tubes in a Vial Tweeter powered by an ultrasonic processor UIS250v (250 W, 2.4 kHz; Hielscher Ultrasonic, Teltow, Germany) to generate fibrillar particles with an average size 50 nm as assessed by TEM analysis. For seeding experiments, either monomeric or fibrillar tau was added directly into the cell culture media to a final concentration of 400 nM. For C-Laurdan experiments, tau was added to cells for 5h with the last 2h C-Laurdan and LysoTracker were spiked into the media. For lysosomal rupture and tau seeding, cells were fixed after 48 hours with tau.

Statistical analysis

Statistical analysis was performed with either GraphPad Prism (GraphPad Software, Version 6h and 10.1.1) or in R (version 4.3.1, with packages ‘nlme’ version 3.1.166, ‘lme4’ version 1.1-35.5, ‘emmeans’ version 1.10.6, ‘dplyr’ version 1.1.4). Data were assessed for normal distribution by Shapiro Normality Test where appropriate. Parametric or non-parametric tests were applied as indicated in the figure legends. Data presentation, sample size (number of replicates, and sample size per experiment and condition), and the applied statistical tests are indicated in the figure legends for each experiment. For all cell culture data, data have been collected in 3 independent experiments with 10 images analyzed in each replicate. For C-Laurdan and LysoTracker, the data was analyzed in R using a two-way mixed-model ANOVA to account for non-independence of measurements acquired from the same experiment and/or image. Models were fitted using the lme4 package. Pairwise comparisons between conditions were performed on estimated marginal means using the emmeans package with Sidak correction for multiple comparisons. Significance levels: non-significant (n.s.) $p > 0.05$, $*p \leq 0.05$, $**p \leq 0.01$, and $***p \leq 0.001$.

Data availability

All data supporting the findings of this study are available within the paper and its supplementary information. *C. elegans* strains and plasmids generated in this study are available upon request.

Acknowledgements

We gratefully acknowledge the technical support of Sarah Wübbel. We extend our gratitude to Dr. Sunil Yeruva for his assistance with the use of the DMI6000 confocal microscope. We appreciate the help of Dr. Hana Nuskova and Dr. Aurelio Teleman (DKFZ, Heidelberg) with the fatty acid conjugation protocol. We thank Dr. Tamara Mikeladze-Dvali (LMU Munich) for her help with generating transgenic animals and for generously providing access to her microinjection system.

The tauP301S-Venus expressing HEK293T cell line was kindly provided by Dr. William A. McEwan (Cambridge University)[37]. The pLenti PGK Puro DEST (w529-2) vector was a gift from Dr. Eric Campeau and Dr. Paul Kaufman[74]. We also thank Dr. Bin Liu and Dr. Marja Jäättelä (University of Copenhagen) for sharing the strain BIJ34 and a pPD49.26 expression plasmid coding for sfGFP::LGALS3 and Dr. Xiaochen Wang (Chinese Academy of Sciences, Beijing) for nematodes expressing the qxIs352 transgene. Some strains were provided by the Caenorhabditis Genetics Center (CGC), which is funded by the NIH Office of Research Infrastructure Programs (P40 OD010440).

Additional information

Author contributions

Conceptualization J.T., C.A.S., C.N.K.

Formal Analysis J.T., C.A.S., N.M.

Funding acquisition R.M., C.N.K.

Investigation J.T., C.A.S., N.M., D.E.

Methodology J.T., C.A.S., N.M., S.B.N.N

Project administration C.N.K.

Resources S.B.N.N.

Supervision R.M., C.N.K.

Visualization J.T., C.N.K.

Writing – original draft J.T., C.A.S., C.N.K.

Writing – review & editing J.T., C.A.S., N.M., D.E., R.M., C.N.K.

Funding

Funder	Grant reference number	Author
Fondation pour la Recherche Médicale (FRM)	ALZ201912009776	Ronald Melki
Alzheimer Forschung Initiative (AFI)	P40 OD010440	Carmen Nussbaum

Author ORCID iDs

Jessica Tittelmeier: https://orcid.org/0000-0002-8202-3702
Carl Alexander Sandhof: https://orcid.org/0000-0001-8692-6987
Ronald Melki: https://orcid.org/0000-0003-0000-7096
Carmen Nussbaum-Krammer: https://orcid.org/0000-0002-8689-1363

Additional files

Supplemental Figures

Table S1

Table S2

References

(1) **Clavaguera F,** Bolmont T, Crowther RA, Abramowski D, Frank S, Probst A, Fraser G, Stalder AK, Beibel M, Staufenbiel M, *et al.* (2009) Transmission and spreading of tauopathy in transgenic mouse brain. *Nature cell biology* **11**:909-909 https://doi.org/10.1038/NCB1901 | PubMed

(2) **Walker LC,** Jucker M (2024) The prion principle and Alzheimer's disease. *Science* **385**:1278-1279 https://doi.org/10.1126/SCIENCE.ADQ5252 | PubMed

(3) **Biel D,** Brendel M, Rubinski A, Buerger K, Janowitz D, Dichgans M, Franzmeier N (2021) ; Alzheimer's Disease Neuroimaging, I. Tau-PET and in vivo Braak-staging as prognostic markers of future cognitive decline in cognitively normal to demented individuals. . *Alzheimer's research & therapy* **13**:137 https://doi.org/10.1186/s13195-021-00880-x | PubMed

(4) **Frost B,** Jacks RL, Diamond MI (2009) Propagation of tau misfolding from the outside to the inside of a cell. *J Biol Chem* **284**:12845-12852 https://doi.org/10.1074/jbc.M808759200 | PubMed

(5) **Sanders DW,** Kaufman SK, DeVos SL, Sharma AM, Mirbaha H, Li A, Barker SJ, Foley AC, Thorpe JR, Serpell LC, *et al.* (2014) Distinct tau prion strains propagate in cells and mice and define different tauopathies. *Neuron* **82**:1271-1288 https://doi.org/10.1016/j.neuron.2014.04.047 | PubMed

(6) **Shrivastava AN,** Redeker V, Pieri L, Bousset L, Renner M, Madiona K, Mailhes-Hamon C, Coens A, Buee L, Hantraye P, *et al.* (2019) Clustering of Tau fibrils impairs the synaptic composition of alpha3-Na(+)/K(+)-ATPase and AMPA receptors. *EMBO J* **38** https://doi.org/10.15252/embj.201899871 | PubMed

(7) **Caballero B,** Wang Y, Diaz A, Tasset I, Juste YR, Stiller B, Mandelkow EM, Mandelkow E, Cuervo AM (2018) Interplay of pathogenic forms of human tau with different autophagic pathways. *Aging cell* **17** https://doi.org/10.1111/acel.12692 | PubMed

(8) **Menzies FM,** Fleming A, Rubinsztein DC (2015) Compromised autophagy and neurodegenerative diseases. *Nat Rev Neurosci* **16**:345-357 https://doi.org/10.1038/nrn3961 | PubMed

(9) **Nixon RA,** Wegiel J, Kumar A, Yu WH, Peterhoff C, Cataldo A, Cuervo AM (2005) Extensive involvement of autophagy in Alzheimer disease: an immuno-electron microscopy study. *J Neuropathol Exp Neurol* **64**:113-122 https://doi.org/10.1093/jnen/64.2.113 | PubMed

(10) **Hou WC,** Massey LA, Rhoades D, Wu Y, Ren W, Frank C, Overkleeft HS, Kelly JW (2024) A PIKfyve modulator combined with an integrated stress response inhibitor to treat lysosomal storage diseases. *Proc Natl Acad Sci U S A* **121**:e2320257121 https://doi.org/10.1073/pnas.2320257121 | PubMed

(11) **Lim SHY,** Hansen M, Kumsta C (2024) Molecular Mechanisms of Autophagy Decline during Aging. *Cells* **13** https://doi.org/10.3390/cells13161364 | PubMed

(12) **Caballero B,** Bourdenx M, Luengo E, Diaz A, Sohn PD, Chen X, Wang C, Juste YR, Wegmann S, Patel B, *et al.* (2021) Acetylated tau inhibits chaperone-mediated autophagy and promotes tau pathology propagation in mice. *Nature communications* **12**:2238 https://doi.org/10.1038/s41467-021-22501-9 | PubMed

(13) **Chen JJ,** Nathaniel DL, Raghavan P, Nelson M, Tian R, Tse E, Hong JY, See SK, Mok SA, Hein MY, *et al.* (2019) Compromised function of the ESCRT pathway promotes endolysosomal escape of tau seeds and propagation of tau aggregation. *J Biol Chem* https://doi.org/10.1074/jbc.RA119.009432 | PubMed

(14) **Flavin WP,** Bousset L, Green ZC, Chu Y, Skarpathiotis S, Chaney MJ, Kordower JH, Melki R, Campbell EM (2017) Endocytic vesicle rupture is a conserved mechanism of cellular invasion by amyloid proteins. *Acta Neuropathol* https://doi.org/10.1007/s00401-017-1722-x | PubMed

(15) **Tuck BJ,** Miller LVC, Katsinelos T, Smith AE, Wilson EL, Keeling S, Cheng S, Vaysburd MJ, Knox C, Tredgett L, *et al.* (2022) Cholesterol determines the cytosolic entry and seeded aggregation of tau. *Cell reports* **39**:110776 https://doi.org/10.1016/j.celrep.2022.110776 | PubMed

(16) **Dimou E,** Katsinelos T, Meisl G, Tuck BJ, Keeling S, Smith AE, Hidari E, Lam JYL, Burke M, et al. (2023) Super-resolution imaging unveils the self-replication of tau aggregates upon seeding. *Cell reports* **42**:112725 https://doi.org/10.1016/j.celrep.2023.112725 | PubMed

(17) **Polanco JC,** Hand GR, Briner A, Li C, Götz J (2021) Exosomes induce endolysosomal permeabilization as a gateway by which exosomal tau seeds escape into the cytosol. *Acta Neuropathol* **141**:235-256 https://doi.org/10.1007/s00401-020-02254-3 | PubMed

(18) **Rose K,** Jepson T, Shukla S, Maya-Romero A, Kampmann M, Xu K, Hurley JH (2024) Tau fibrils induce nanoscale membrane damage and nucleate cytosolic tau at lysosomes. *Proc Natl Acad Sci U S A* **121**:e2315690121 https://doi.org/10.1073/pnas.2315690121 | PubMed

(19) **Kroemer G,** Jaattela M (2005) Lysosomes and autophagy in cell death control. *Nature reviews. Cancer* **5**:886-897 https://doi.org/10.1038/nrc1738 | PubMed

(20) **Sandhof CA,** Martin N, Tittelmeier J, Schlueter A, Pezzali M, Schoendorf DC, Lange T, Reinhardt P, Ried JS, Liang S, *et al.* (2025) A novel C. elegans model for MAPT/Tau spreading reveals genes critical for endolysosomal integrity and seeded MAPT/Tau aggregation. *Autophagy* https://doi.org/10.1080/15548627.2025.2551676 | PubMed

(21) **Breslow DK,** Weissman JS (2010) Membranes in balance: mechanisms of sphingolipid homeostasis. *Mol Cell* **40**:267-279 https://doi.org/10.1016/j.molcel.2010.10.005 | PubMed

(22) **Jimenez-Rojo N,** Leonetti MD, Zoni V, Colom A, Feng S, Iyengar NR, Matile S, Roux A, Vanni S, Weissman JS, *et al.* (2020) Conserved Functions of Ether Lipids and Sphingolipids in the Early Secretory Pathway. *Curr Biol* **30**:3775-3787.e3777. https://doi.org/10.1016/j.cub.2020.07.059 | PubMed

(23) **Gault CR,** Obeid LM, Hannun YA (2010) An overview of sphingolipid metabolism: from synthesis to breakdown. *Adv Exp Med Biol* **688**:1-23 https://doi.org/10.1007/978-1-4419-6741-1_1 | PubMed

(24) **Futerman AH,** Hannun YA (2004) The complex life of simple sphingolipids. *EMBO Rep* **5**:777-782 https://doi.org/10.1038/sj.embor.7400208 | PubMed

(25) **Czubowicz K,** Jesko H, Wencel P, Lukiw WJ, Strosznajder RP (2019) The Role of Ceramide and Sphingosine-1-Phosphate in Alzheimer's Disease and Other Neurodegenerative Disorders. *Mol Neurobiol* **56**:5436-5455 https://doi.org/10.1007/s12035-018-1448-3 | PubMed

(26) **van Echten-Deckert G,** Walter J (2012) Sphingolipids: critical players in Alzheimer's disease. *Prog Lipid Res* **51**:378-393 https://doi.org/10.1016/j.plipres.2012.07.001 | PubMed

(27) **Huotari J,** Helenius A (2011) Endosome maturation. *EMBO J* **30**:3481-3500 https://doi.org/10.1038/emboj.2011.286 | PubMed

(28) **Yong J,** Villalta JE, Vu N, Kukurugya MA, Olsson N, Lopez MP, Lazzari-Dean JR, Hake K, McAllister FE, Bennett BD, *et al.* (2024) Impairment of lipid homeostasis causes lysosomal accumulation of endogenous protein aggregates through ESCRT disruption. *eLife* **12** https://doi.org/10.7554/eLife.86194 | PubMed

(29) **Aits S,** Kricker J, Liu B, Ellegaard AM, Hamalisto S, Tvingsholm S, Corcelle-Termeau E, Hogh S, Farkas T, Holm Jonassen A, *et al.* (2015) Sensitive detection of lysosomal membrane permeabilization by lysosomal galectin puncta assay. *Autophagy* **11**:1408-1424 https://doi.org/10.1080/15548627.2015.1063871 | PubMed

(30) **Hanel V,** Pendleton C, Witting M (2019) The sphingolipidome of the model organism Caenorhabditis elegans. *Chem Phys Lipids* **222**:15-22 https://doi.org/10.1016/j.chemphyslip.2019.04.009 | PubMed

(31) **Cheng X,** Jiang X, Tam KY, Li G, Zheng J, Zhang H (2019) Sphingolipidomic Analysis of C. elegans reveals Development- and Environment-dependent Metabolic Features. *Int J Biol Sci* **15**:2897-2910 https://doi.org/10.7150/ijbs.30499 | PubMed

(32) **D'Auria L,** Bongarzone ER (2016) Fluid levity of the cell: Role of membrane lipid architecture in genetic sphingolipidoses. *J Neurosci Res* **94**:1019-1024 https://doi.org/10.1002/jnr.23750 | PubMed

(33) **Liu B,** Du H, Rutkowski R, Gartner A, Wang X (2012) LAAT-1 is the lysosomal lysine/arginine transporter that maintains amino acid homeostasis. *Science* **337**:351-354 https://doi.org/10.1126/science.1220281 | PubMed

(34) **Morck C,** Olsen L, Kurth C, Persson A, Storm NJ, Svensson E, Jansson JO, Hellqvist M, Enejder A, Faergeman NJ, *et al.* (2009) Statins inhibit protein lipidation and induce the unfolded protein response in the non-sterol producing nematode Caenorhabditis elegans. *Proc Natl Acad Sci U S A* **106**:18285-18290 https://doi.org/10.1073/pnas.0907117106 | PubMed

(35) **Owen DM,** Rentero C, Magenau A, Abu-Siniyeh A, Gaus K (2011) Quantitative imaging of membrane lipid order in cells and organisms. *Nat Protoc* **7**:24-35 https://doi.org/10.1038/nprot.2011.419 | PubMed

(36) **Barucha-Kraszewska J,** Kraszewski S, Ramseyer C (2013) Will C-Laurdan dethrone Laurdan in fluorescent solvent relaxation techniques for lipid membrane studies?. *Langmuir* **29**:1174-1182 https://doi.org/10.1021/la304235r | PubMed

(37) **McEwan WA,** Falcon B, Vaysburd M, Clift D, Oblak AL, Ghetti B, Goedert M, James LC (2017) Cytosolic Fc receptor TRIM21 inhibits seeded tau aggregation. *Proc Natl Acad Sci U S A* **114**:574-579 https://doi.org/10.1073/pnas.1607215114 | PubMed

(38) **Nachman E,** Wentink AS, Madiona K, Bousset L, Katsinelos T, Allinson K, Kampinga H, McEwan WA, Jahn TR, Melki R, *et al.* (2020) Disassembly of Tau fibrils by the human Hsp70 disaggregation machinery generates small seeding-competent species. *J Biol Chem* **295**:9676-9690 https://doi.org/10.1074/jbc.RA120.013478 | PubMed

(39) **Ruiz M,** Devkota R, Kaper D, Ruhanen H, Busayavalasa K, Radovic U, Henricsson M, Kakela R, Boren J, Pilon M (2023) AdipoR2 recruits protein interactors to promote fatty acid elongation and membrane fluidity. *J Biol Chem* **299**:104799 https://doi.org/10.1016/j.jbc.2023.104799 | PubMed

(40) **Zhang Y,** Wang H, Zhang J, Hu Y, Zhang L, Wu X, Su X, Li T, Zou X, Liang B (2016) The cytochrome b5 reductase HPO-19 is required for biosynthesis of polyunsaturated fatty acids in Caenorhabditis elegans. *Biochim Biophys Acta* **1861**:310-319 https://doi.org/10.1016/j.bbalip.2016.01.009 | PubMed

(41) **Yong J,** Villalta JE, Vu N, Kukurugya MA, Olsson N, López MP, Lazzari-Dean JR, Hake K, McAllister FE, Bennett BD, *et al.* (2024) Impairment of lipid homeostasis causes lysosomal accumulation of endogenous protein aggregates through ESCRT disruption. *eLife* **12** https://doi.org/10.7554/ELIFE.86194 | PubMed

(42) **Li Y,** Zhang J, Li M, Yang L, Wang X (2026) Sphingosine kinase SPHK-1 maintains sphingolipid metabolism to protect lysosome membrane integrity in C. elegans. *Mol Biol Cell* **37**:ar1 https://doi.org/10.1091/mbc.E25-04-0182 | PubMed

(43) **Yoon JH,** Seo Y, Jo YS, Lee S, Cho E, Cazenave-Gassiot A, Shin YS, Moon MH, An HJ, Wenk MR, *et al.* (2022) Brain lipidomics: From functional landscape to clinical significance. *Sci Adv* **8**:eadc9317 https://doi.org/10.1126/sciadv.adc9317 | PubMed

(44) **Hornemann T** (2021) Mini review: Lipids in Peripheral Nerve Disorders. *Neurosci Lett* **740** https://doi.org/10.1016/j.neulet.2020.135455 | PubMed

(45) **Uranbileg B,** Isago H, Sakai E, Kubota M, Saito Y, Kurano M (2024) Alzheimer's disease manifests abnormal sphingolipid metabolism. *Front Aging Neurosci* **16** https://doi.org/10.3389/fnagi.2024.1368839 | PubMed

(46) **Corder EH,** Saunders AM, Strittmatter WJ, Schmechel DE, Gaskell PC, Small GW, Roses AD, Haines JL, Pericak-Vance MA (1993) Gene dose of apolipoprotein E type 4 allele and the risk of Alzheimer's disease in late onset families. *Science* **261**:921-923 https://doi.org/10.1126/science.8346443 | PubMed

(47) **Kosicek M,** Zetterberg H, Andreasen N, Peter-Katalinic J, Hecimovic S (2012) Elevated cerebrospinal fluid sphingomyelin levels in prodromal Alzheimer's disease. *Neurosci Lett* **516**:302-305 https://doi.org/10.1016/j.neulet.2012.04.019 | PubMed

(48) **Fabri J,** de Sa NP, Malavazi I, Del Poeta M (2020) The dynamics and role of sphingolipids in eukaryotic organisms upon thermal adaptation. *Prog Lipid Res* **80** https://doi.org/10.1016/j.plipres.2020.101063 | PubMed

(49) **Romanauska A,** Kohler A (2023) Lipid saturation controls nuclear envelope function. *Nat Cell Biol* **25**:1290-1302 https://doi.org/10.1038/s41556-023-01207-8 | PubMed

(50) **Harayama T,** Riezman H (2018) Understanding the diversity of membrane lipid composition. *Nat Rev Mol Cell Biol* **19**:281-296 https://doi.org/10.1038/nrm.2017.138 | PubMed

(51) **Elias RD,** O'Neill RT, Demiralp II, Allen S, Serwas D, Siems H, Montabana EA, Ash C, Yacoubian DA, Lederberg OL, *et al.* (2025) Cathepsin C-Catalyzed Ligation Generates Intralysosomal Amyloid Fibrils from Dipeptide Esters. *bioRxiv* https://doi.org/10.64898/2025.12.23.696283 | PubMed

(52) **Li D,** Zhang W, Medina M, Stuke JFM, Schwarz A, Brill J, Brenner J, Kraus F, Ohlerich S, Lizarrondo J, *et al.* (2026) Cathepsin-dependent amyloid formation drives mechanical rupture of lysosomal membranes. *bioRxiv* https://doi.org/10.64898/2026.01.17.700056 | PubMed

(53) **Calixto A,** Chelur D, Topalidou I, Chen X, Chalfie M (2010) Enhanced neuronal RNAi in C. elegans using SID-1. *Nat Methods* **7**:554-559 https://doi.org/10.1038/nmeth.1463 | PubMed

(54) **Tittelmeier J,** Nussbaum-Krammer C (2025) Broken Balance: Emerging Cross-Talk Between Proteostasis and Lipostasis in Neurodegenerative Diseases. *Cells* **14** https://doi.org/10.3390/cells14110845 | PubMed

(55) **Rakhra V,** Galappaththy SL, Bulchandani S, Cabandugama PK (2020) Obesity and the Western Diet: How We Got Here. *Mo Med* **117**:536-538 PubMed

(56) **Wretlind A,** Xu J, Chen W, Velayudhan L, Ashton NJ, Zetterberg H, Proitsi P, Legido-Quigley C (2025) Lipid profiling reveals unsaturated lipid reduction in women with Alzheimer's disease. *Alzheimers Dement* **21**:e70512 https://doi.org/10.1002/alz.70512 | PubMed

(57) **Snowden SG,** Ebshiana AA, Hye A, An Y, Pletnikova O, O'Brien R, Troncoso J, Legido-Quigley C, Thambisetty M (2017) Association between fatty acid metabolism in the brain and Alzheimer disease neuropathology and cognitive performance: A nontargeted metabolomic study. *PLoS Med* **14**:e1002266 https://doi.org/10.1371/journal.pmed.1002266 | PubMed

(58) **Bischoff-Ferrari HA,** Gangler S, Wieczorek M, Belsky DW, Ryan J, Kressig RW, Stahelin HB, Theiler R, Dawson-Hughes B, Rizzoli R, *et al.* (2025) Individual and additive effects of vitamin D, omega-3 and exercise on DNA methylation clocks of biological aging in older adults from the DO-HEALTH trial. *Nat Aging* https://doi.org/10.1038/s43587-024-00793-y | PubMed

(59) **Shinto L,** Quinn J, Montine T, Dodge HH, Woodward W, Baldauf-Wagner S, Waichunas D, Bumgarner L, Bourdette D, Silbert L, *et al.* (2014) A randomized placebo-controlled pilot trial of omega-3 fatty acids and alpha lipoic acid in Alzheimer's disease. *J Alzheimers Dis* **38**:111-120 https://doi.org/10.3233/JAD-130722 | PubMed

(60) **Wood AHR,** Chappell HF, Zulyniak MA (2022) Dietary and supplemental long-chain omega-3 fatty acids as moderators of cognitive impairment and Alzheimer's disease. *Eur J Nutr* **61**:589-604 https://doi.org/10.1007/s00394-021-02655-4 | PubMed

(61) **Brenner S** (1974) The genetics of Caenorhabditis elegans. *Genetics* **77**:71-94 https://doi.org/10.1093/genetics/77.1.71 | PubMed

(62) **Svensk E,** Stahlman M, Andersson CH, Johansson M, Boren J, Pilon M (2013) PAQR-2 regulates fatty acid desaturation during cold adaptation in C. elegans. *PLoS Genet* **9**:e1003801 https://doi.org/10.1371/journal.pgen.1003801 | PubMed

(63) **Ruiz M,** Bodhicharla R, Svensk E, Devkota R, Busayavalasa K, Palmgren H, Stahlman M, Boren J, Pilon M (2018) Membrane fluidity is regulated by the C. elegans transmembrane protein FLD-1 and its human homologs TLCD1/2. *eLife* **7** https://doi.org/10.7554/eLife.40686 | PubMed

(64) **Devkota R,** Svensk E, Ruiz M, Stahlman M, Boren J, Pilon M (2017) The adiponectin receptor AdipoR2 and its Caenorhabditis elegans homolog PAQR-2 prevent membrane rigidification by exogenous saturated fatty acids. *PLoS Genet* **13**:e1007004 https://doi.org/10.1371/journal.pgen.1007004 | PubMed

(65) **Sandhof CA,** Hoppe SO, Druffel-Augustin S, Gallrein C, Kirstein J, Voisine C, Nussbaum-Krammer C (2020) Reducing INS-IGF1 signaling protects against non-cell autonomous vesicle rupture caused by SNCA spreading. *Autophagy* **16**:878-899 https://doi.org/10.1080/15548627.2019.1643657 | PubMed

(66) **Devkota R,** Pilon M (2018) FRAP: A Powerful Method to Evaluate Membrane Fluidity in Caenorhabditis elegans. *Bio Protoc* **8**:e2913 https://doi.org/10.21769/BioProtoc.2913 | PubMed

(67) **Svensk E,** Devkota R, Stahlman M, Ranji P, Rauthan M, Magnusson F, Hammarsten S, Johansson M, Boren J, Pilon M (2016) Caenorhabditis elegans PAQR-2 and IGLR-2 Protect against Glucose Toxicity by Modulating Membrane Lipid Composition. *PLoS Genet* **12**:e1005982 https://doi.org/10.1371/journal.pgen.1005982 | PubMed

(68) **Chalfie M,** Sulston JE, White JG, Southgate E, Thomson JN, Brenner S (1985) The neural circuit for touch sensitivity in Caenorhabditis elegans. *J Neurosci* **5**:956-964 https://doi.org/10.1523/jneurosci.05-04-00956.1985 | PubMed

(69) **Jeong JH,** Han JS, Jung Y, Lee SM, Park SH, Park M, Shin MG, Kim N, Kang MS, Kim S, *et al.* (2023) A new AMPK isoform mediates glucose-restriction induced longevity non-cell autonomously by promoting membrane fluidity. *Nature communications* **14**:288 https://doi.org/10.1038/s41467-023-35952-z | PubMed

(70) **Oliveira AF,** Cunha DA, Ladriere L, Igoillo-Esteve M, Bugliani M, Marchetti P, Cnop M (2015) In vitro use of free fatty acids bound to albumin: A comparison of protocols. *Biotechniques* **58**:228-233 https://doi.org/10.2144/000114285 | PubMed

(71) **Cousin SP,** Hugl SR, Wrede CE, Kajio H, Myers MG, Rhodes CJ (2001) Free fatty acid-induced inhibition of glucose and insulin-like growth factor I-induced deoxyribonucleic acid synthesis in the pancreatic beta-cell line INS-1. *Endocrinology* **142**:229-240 https://doi.org/10.1210/endo.142.1.7863 | PubMed

(72) **Nuskova H,** Cortizo FG, Schwenker LS, Sachsenheimer T, Diakonov EE, Tiebe M, Schneider M, Lohbeck J, Reid C, Kopp-Schneider A, *et al.* (2023) Competition for cysteine acylation by C16:0 and C18:0 derived lipids is a global phenomenon in the proteome. *J Biol Chem* **299**:105088 https://doi.org/10.1016/j.jbc.2023.105088 | PubMed

(73) **Tardivel M,** Begard S, Bousset L, Dujardin S, Coens A, Melki R, Buee L, Colin M (2016) Tunneling nanotube (TNT)-mediated neuron-to neuron transfer of pathological Tau protein assemblies. *Acta neuropathologica communications* **4**:117 https://doi.org/10.1186/s40478-016-0386-4 | PubMed

(74) **Campeau E,** Ruhl VE, Rodier F, Smith CL, Rahmberg BL, Fuss JO, Campisi J, Yaswen P, Cooper PK, Kaufman PD (2009) A versatile viral system for expression and depletion of proteins in mammalian cells. *PLoS One* **4**:e6529 https://doi.org/10.1371/journal.pone.0006529 | PubMed

(75) **Chitwood DJ,** Lusby WR, Thompson MJ, Kochansky JP, Howarth OW (1995) The glycosylceramides of the nematode Caenorhabditis elegans contain an unusual, branched-chain sphingoid base. *Lipids* **30**:567-573 https://doi.org/10.1007/BF02537032 | PubMed

(76) **Zhang H,** Abraham N, Khan LA, Hall DH, Fleming JT, Gobel V (2011) Apicobasal domain identities of expanding tubular membranes depend on glycosphingolipid biosynthesis. *Nat Cell Biol* **13**:1189-1201 https://doi.org/10.1038/ncb2328 | PubMed

(77) **Zhu H,** Shen H, Sewell AK, Kniazeva M, Han M (2013) A novel sphingolipid-TORC1 pathway critically promotes postembryonic development in Caenorhabditis elegans. *eLife* **2**:e00429 https://doi.org/10.7554/eLife.00429 | PubMed

(78) **Scholz J,** Helmer PO, Nicolai MM, Bornhorst J, Hayen H (2021) Profiling of sphingolipids in Caenorhabditis elegans by two-dimensional multiple heart-cut liquid chromatography - mass spectrometry. *J Chromatogr A* **1655**:462481 https://doi.org/10.1016/j.chroma.2021.462481 | PubMed

Peer reviews

Reviewer #1 (Public review):

Summary:

In this study, Tittelmeier et al. explored the role of sphingolipid metabolism in maintaining endolysosomal membrane integrity and its downstream effects on tau aggregation and toxicity, using both worms and human cell models. The authors showed that knockdown of sphingolipid metabolism genes reduced endolysosomal membrane fluidity, as revealed by FRAP and C-Laurdan imaging, leading to increased vesicle rupture. Furthermore, tau aggregates accumulated in endolysosomes and exacerbated membrane rigidity and damage, promoting seeded tau aggregation, likely by enabling tau seed escape into the cytosol. Importantly, unsaturated fatty acid supplementation restored membrane fluidity, suppressed tau propagation, and alleviated neurotoxicity in C. elegans. These findings provide insight

into how lipid dysregulation contributes to tau pathology and highlight membrane fluidity restoration as a potential therapeutic avenue for Alzheimer's disease.

Strengths:

The study addresses the connection between sphingolipid metabolism, endolysosomal membrane integrity, and tau pathology, which is a relevant topic in the context of Alzheimer's disease and related tauopathies.

The use of both C. elegans and human cell models provides cross-species perspectives that help frame the findings in a broader biological context.

The combination of FRAP and C-Laurdan dye imaging offers a biophysical approach to investigate changes in membrane properties, which is a technically interesting aspect of the study.

The observation that unsaturated fatty acid supplementation can modulate membrane fluidity and influence tau-related phenotypes adds an element of potential therapeutic interest.

The study presents multiple experimental approaches to address the proposed mechanism, and efforts were made to examine both membrane behavior and tau aggregation dynamics.

Comments on revised version:

I thank the authors for their thorough revisions and detailed responses. All of my previous concerns have been satisfactorily addressed, and I have no further comments.

https://doi.org/10.7554/eLife.106865.2.sa3

Reviewer #2 (Public review):

Tittelmeier et al. investigated the role of sphingolipid (SL) metabolism in the maintenance of endolysosomal vesicle integrity. They find that both impaired SL biosynthesis and degradation in C. elegans decreases the fluidity of endolysosomal membranes and promotes their rupture, while it has little effect on plasma membrane fluidity. Endolysosomal membrane fluidity is also negatively affected in human cells upon knockdown (KD) of a gene (SPHK2) involved in the SL degradation pathway. Aggregated forms of tau in both models (C. elegans and human cells) can also cause rigidification of the endolysosomal membrane, with SL homeostasis disruption having an additive effect, exacerbating endolysosomal rupture. Notably, KD of SPHK2 also increased the formation of tau foci, suggesting that compromised endolysosomal integrity may promote tau aggregation. These data provide a clearer understanding of how genetic manipulation of SL metabolism affects endolysosomal membranes and their rigidification in the context of tau aggregation. Supplementation of polyunsaturated fatty acids (PUFAs), which has a beneficial effect on Alzheimer's patients, improved membrane fluidity and reduced tau propagation in human cells and tau-associated neurotoxicity in C. elegans, suggesting a possible mechanism of action.

Comments on revised version:

The authors have:

Corrected editorial errors (Points 1 and 2).

Clarified the experimental rationale, added new data to rule out alternative explanation, and improved the presentation of the C. elegans model (Point 3).

Provided experimental evidence and appropriate discussion regarding the specificity and broader physiological context of SL gene knockdown effects (Point 4).

Overall, the authors' responses are thorough, supported by new data where appropriate, and demonstrate a clear understanding of the concerns raised. All points raised have been satisfactorily resolved.

https://doi.org/10.7554/eLife.106865.2.sa2

Reviewer #3 (Public review):

Summary:

The authors set off with an analysis of the lysosomal integrity upon knockdown of genes of the sphingolipid metabolic pathway that they identified in a previous work of an RNA screen using a new C.elegans Tau model. They then used cell culture and C.elegans experiments to study the link between lysosomal rupture and Tau propagation.

Strengths:

The authors use two complementary model systems and used probes to assess membrane rigidity that allow a quick assessment of the membrane dynamics and offer the opportunity to treat the cells with lipids, RNAi. Tau seeds etc.

Comments on revised version:

The authors have addressed the majority of my critical comments and thus I support the manuscript.

They have still not analysed the knockdown efficiencies of their RNAi experiments. But this is their choice.

The other publication establishing their Tau model is meanwhile published and there is no disconnect anymore between the model their analysis builds on.

https://doi.org/10.7554/eLife.106865.2.sa1

Author response:

The following is the authors' response to the original reviews.

> ***Public Reviews:***
>
> ***Reviewer #1 (Public review):***
>
> *Summary:*
>
> *In this study, Tittelmeier et al. explored the role of sphingolipid metabolism in maintaining endolysosomal membrane integrity and its downstream effects on tau aggregation and toxicity, using both worms and human cell models. The authors showed that knockdown of sphingolipid metabolism genes reduced endolysosomal membrane fluidity, as revealed by FRAP and C-Laurdan imaging, leading to increased vesicle rupture. Furthermore, tau aggregates accumulated in endolysosomes and exacerbated membrane rigidity and damage, promoting seeded tau aggregation, likely by enabling tau seed escape into the cytosol. Importantly, unsaturated fatty acid supplementation restored membrane fluidity, suppressed tau propagation, and alleviated neurotoxicity in C. elegans. These findings provide insight into how lipid dysregulation contributes to tau*

> *pathology and highlight membrane fluidity restoration as a potential therapeutic avenue for Alzheimer's disease.*
>
> *Strengths:*
>
> *The study addresses the connection between sphingolipid metabolism, endolysosomal membrane integrity, and tau pathology, which is a relevant topic in the context of Alzheimer's disease and related tauopathies.*
>
> *The use of both C. elegans and human cell models provides cross-species perspectives that help frame the findings in a broader biological context.*
>
> *The combination of FRAP and C-Laurdan dye imaging offers a biophysical approach to investigate changes in membrane properties, which is a technically interesting aspect of the study.*
>
> *The observation that unsaturated fatty acid supplementation can modulate membrane fluidity and influence tau-related phenotypes adds an element of potential therapeutic interest.*
>
> *The study presents multiple experimental approaches to address the proposed mechanism, and efforts were made to examine both membrane behavior and tau aggregation dynamics.*

We thank the reviewer for this positive assessment of the study.

> *Weaknesses:*
>
> *In Figure 3, the authors used C-Laurdan imaging to assess membrane fluidity and showed that knockdown of SPHK2, the human ortholog of sphk-1, led to increased membrane rigidity. However, the authors did not co-stain with a lysosomal marker, making it unclear whether the observed effect is specific to lysosomal membranes or reflects general membrane changes. Co-staining with LysoTracker or applying segmentation masks to isolate lysosomal signals would significantly improve interpretation.*

We agree with the reviewer that it is important to isolate lysosomal signals for interpreting the C-Laurdan data. We therefore repeated and extended the C-Laurdan experiments in combination with LysoTracker staining and selectively analyzed LysoTracker-positive regions. These analyses showed pronounced increases in GP values in LysoTracker-positive vesicles after SPHK2 knockdown, supporting the conclusion that SPHK2 depletion increases endolysosomal membrane rigidity. We also performed LysoTracker-based analysis in the tau-fibril and fatty-acid experiments to better assess lysosome-associated membrane properties (see new and updated Figures 3B-E, Figures 5A and B, Figures S3A, B, F, G, Figures S4A-F, and Figures S5A-D for details). The respective Results sections have been revised accordingly.

> *Line 173 states that Lipofectamine 2000 increases membrane fluidity based on GP index changes, but this is incorrect. A higher GP index indicates increased membrane order (i.e., reduced fluidity), so the statement should be revised. Additionally, Lipofectamine 2000 can itself alter membrane rigidity, posing a risk of false-positive interpretations. To confirm the role of SPHK2 in this phenotype, the authors should use a CRISPR/Cas9 knockout model instead of relying solely on siRNA transfection, which may be confounded by the delivery reagent. Without lysosomal co-staining and SPHK2 KO validation, the authors cannot conclusively claim that SPHK2 loss affects endolysosomal membrane integrity.*

We thank the reviewer for pointing out the incorrect wording regarding Lipofectamine. A higher GP index indicates increased membrane order/rigidity, not increased fluidity. Since

the revised main figure now includes the SH-SY5Y data (Figure 3A-D), in which Lipofectamine alone did not significantly alter GP values (see Figure S3A, B), we removed the misleading statement from the Results.

We also agree that Lipofectamine can affect membrane properties and therefore needs to be carefully controlled. In all siRNA-mediated experiments, SPHK2 siRNA was compared to a matched control siRNA condition exposed to the same transfection reagent. We state in the Methods that cells were transfected with either SPHK2 or scrambled control siRNA and that the medium was exchanged after 6 h "to minimize lipofectamine impact on the endolysosomal system". Thus, the effect attributed to SPHK2 KD is assessed relative to the appropriate Lipofectamine-containing control condition.

Importantly, we have now added lysosomal co-staining to address the reviewer's concern about compartment specificity. This analysis showed that SPHK2 KD resulted in a pronounced increase in GP values within LysoTracker-positive compartments, demonstrating increased membrane rigidity at lysosomes. Thus, the revised data support the conclusion that SPHK2 KD increases lysosome-associated membrane rigidity, rather than only causing nonspecific effects on other cellular membranes.

We also clarified the relationship between the current siRNA-based assay and our previous CRISPR inhibition-based analysis. In the revised Results, we now write: "While SPHK2 KD alone significantly increased galectin puncta above the matched control, its effect was more modest than in our previous CRISPR inhibition-based analysis [20]. This difference likely stems from the earlier readout required for the combined siRNA/tau fibril assay, when transient Lipofectamine-associated effects still increased the control background."

This addresses why the SPHK2 KD effect appears smaller in the current siRNA/tau-fibril assay than in our previous CRISPR inhibition-based analysis. The previous study, which is now peer-reviewed and published in the journal Autophagy, used a CRISPR inhibition-based strategy to reduce SPHK2 levels, which resulted in a highly significant increase in sfGFP-LGALS3 foci formation compared to the control [1]. Thus, the SPHK2 phenotype is not supported solely by the current siRNA experiment.

In addition, we sought to genetically validate the RNAi phenotypes using mutant strains. However, mutant strains were not available for all sphingolipid metabolism hits analyzed in this study. We therefore used the *sphk-1* mutant strain available at CGC (CZ24969; sphk-1(ju831)) to validate one of the key SL metabolism hits independently of RNAi. The revised manuscript states: "As genetic validation independent of RNAi, we tested an available sphk-1 mutant strain, which also showed a robust increase in hypodermal sfGFP::LGALS3 foci (Figure S1A)." This result supports the conclusion that genetic perturbation of sphingosine kinase activity compromises endolysosomal integrity *in vivo*.

Together, the revised manuscript addresses the reviewer's concerns by correcting the GP interpretation, controlling the siRNA experiments against matched Lipofectamine-treated controls, adding LysoTracker-based lysosome-associated C-Laurdan analysis, relating the current siRNA data to our previous CRISPR inhibition-based analysis, and providing genetic validation for the available *sphk-1* mutant.

> *The section titled "Fibrillar tau increases membrane rigidity and exacerbates endolysosomal damage" (lines 177-215) requires substantial revision. The narrative jumps abruptly between worms and cell models, making it hard to follow the logic. The use of the F3ΔK281::mCherry strain is introduced without explanation or context. It is unclear whether this strain is relevant to lysosomal membrane rupture, as no reference or justification is provided. The authors should clarify whether this reporter is intended to detect lysosomal membrane permeabilization (LMP). If so, it would be more appropriate to use established LMP reporters, such as lysosome-targeted fluorescent sensors,*

> *galectin-based reporters, or dextran leakage assays. Based on the current data in Figure 3G, it is difficult to draw firm conclusions regarding membrane rupture levels.*

We agree that this section required clarification, and we have substantially revised the Results to improve the logic and separation between model systems.

First, we now introduce the *C. elegans* reporter strain earlier in the manuscript, in the first Results section. In the revised text, we explain both the tau construct and the actual lysosomal damage reporter: "In this strain, endolysosomal membrane damage is monitored in the hypodermis by expression of human galectin-3 fused to superfolder-GFP (sfGFP::LGALS3). The animals also express an aggregation-prone tau fragment fused to mCherry (F3ΔK281::mCherry) in touch receptor neurons, which is transmitted to the hypodermis, as described previously [20]." We also clarify the principle of the Galectin reporter: "Under steady-state conditions, sfGFP::LGALS3 remains diffusely distributed throughout the cytosol. Upon endolysosomal damage, luminal β-galactosides become exposed and recruit sfGFP::LGALS3 into visible puncta, providing a sensitive readout of vesicle rupture." Thus, F3ΔK281::mCherry is not the reporter for lysosomal membrane permeabilization; the membrane-damage readout is sfGFP::LGALS3 puncta formation.

Second, we reorganized the manuscript to separate the human cell experiments from the *C. elegans* experiments more clearly. The revised section "Fibrillar tau and SPHK2 KD act in concert to exacerbate endolysosomal damage and seeded tau aggregation" now focuses on human cell data. The *C. elegans* experiments are now presented in a separate section, "Tau transmission sensitizes endolysosomal membranes to sphingolipid perturbations *in vivo*." We believe that this revised structure now clearly distinguishes the role of the Galectin reporter from the tau transmission model, separates the human cell and *C. elegans* data, and avoids the abrupt transitions between model systems noted by the reviewer.

> *To support the conclusion that sphingolipid metabolism gene knockdown alters membrane properties, the study would benefit from direct lipidomic analysis. Measuring changes in sphingolipid profiles in both C. elegans and cell models would provide biochemical evidence for the proposed disruption of lipid homeostasis. Given the availability of lipidomics platforms, this type of analysis should be feasible in both worms and human cells and would significantly strengthen the mechanistic claims regarding membrane fluidity and integrity.*

Because we did not perform lipidomics in the present study, we have revised the wording throughout the manuscript to avoid implying that we directly measured lipid composition. Instead, we now refer to "genetic perturbation/disruption of sphingolipid metabolism" or "knockdown of enzymes involved in sphingolipid metabolism" when describing our experimental interventions.

We agree that lipidomic analyses will be important in future studies to define how perturbation of sphingolipid metabolism changes lipid composition in *C. elegans* and human cells. However, lipidomics itself would not directly establish which lipid changes causally drive the membrane rigidification observed in our study. Membrane fluidity is a biophysical property determined by the combined composition of the membrane, including lipid abundance, saturation, acyl-chain length, head groups, sterol content, and membrane-associated proteins. Thus, even if lipidomics identified changes in sphingolipid profiles, these changes could not be directly translated into a predictable effect on membrane fluidity without additional biophysical validation, using Laurdan dye imaging or FRAP. Moreover, whole-cell or whole-animal lipidomics would not resolve whether the relevant lipid changes occur specifically at endolysosomal membranes, which are the focus of our study.

We have now clarified this point in the Discussion. Specifically, we state that "even detailed lipidomics would not by itself identify which lipid changes are responsible for the observed

membrane rigidification" and that future lysosome-enriched or organelle-specific lipidomic approaches should be combined with direct manipulation of candidate lipid species, followed by measurements of membrane fluidity and rupture, to determine which lipid changes causally contribute to endolysosomal membrane rigidification. In the present study, we therefore focused on direct quantitative biophysical readouts of membrane properties in *C. elegans*. We used FRAP of the lysosomal membrane protein LAAT-1::mCherry to assess lateral mobility within lysosomal membranes and showed that knockdown of sphingolipid-metabolism genes increased the time to half-maximal recovery, indicating reduced lysosomal membrane fluidity. Notably, knockdown of genes involved in both sphingolipid biosynthesis and sphingolipid degradation increased membrane rigidity. This makes it unlikely that the observed rigidification is caused by accumulation or depletion of a single shared lipid species. Rather, perturbations at different steps of sphingolipid metabolism may lead to distinct lipidomic changes that nevertheless converge on a common biophysical outcome: reduced endolysosomal membrane fluidity. In parallel, we used C-Laurdan imaging to quantify membrane order and found that SPHK2 knockdown in SH-SY5Y human neuroblastoma cells increased GP values, consistent with increased membrane rigidity. Two-channel thresholding of LysoTracker-positive compartments further showed that SPHK2 knockdown increased GP values in lysosome-associated regions.

Thus, although lipidomics will be valuable to define the underlying lipid changes in future work, the current data already provide convergent quantitative evidence from independent membrane-fluidity readouts across *C. elegans* and human cell models. This cross-model consistency strengthens the robustness and reproducibility of the central conclusion that perturbation of sphingolipid metabolism alters endolysosomal membrane properties and promotes membrane rupture.

> *The conclusions of the study rely heavily on imaging-based assays, including FRAP, C-Laurdan, and fluorescence microscopy. While these approaches provide valuable spatial and qualitative insights, they are inherently indirect and subject to interpretive limitations. To strengthen the mechanistic claims, the authors should incorporate additional biochemical or quantitative approaches. For example, lipidomics would allow direct measurement of membrane lipid composition changes, and western blotting or quantitative proteomics could assess levels of membrane-associated proteins involved in endolysosomal function or stress responses. Including such data would significantly improve the robustness and reproducibility of the study's conclusions.*

We agree that lipidomic and proteomic analyses will be important in future studies to define which sphingolipid species and/or membrane-associated proteins contribute to the observed rigidification of endolysosomal membranes. In response to this point, we have revised the wording throughout the manuscript to more precisely distinguish our experimental interventions from inferred changes in lipid composition. Because we did not directly measure lipid composition in the present study, we now refer more specifically to "genetic perturbation/disruption of sphingolipid metabolism" or "knockdown of enzymes involved in sphingolipid metabolism" when describing our data, rather than implying that global sphingolipid homeostasis was directly quantified. We retain "sphingolipid imbalance" only in interpretive or model-based statements where appropriate.

However, we respectfully disagree that the current data are only qualitative. FRAP and C-Laurdan GP imaging are established quantitative biophysical approaches: FRAP provides quantitative parameters such as the time to half-maximal recovery and the mobile fraction, whereas C-Laurdan GP provides a ratiometric measurement of membrane lipid order and packing. Similarly, the Galectin puncta assay is an established quantitative readout of lysosomal membrane permeabilization. Thus, while these approaches are imaging-based, they provide quantitative readouts of membrane mobility, membrane order, and membrane rupture, respectively.

We also note that lipidomic and proteomic profiling, although valuable, would not by itself establish which lipid or protein changes causally drive the membrane rigidification observed in our study. Membrane fluidity is an emergent biophysical property determined by the combined composition of the membrane, including lipid abundance, saturation, acyl-chain length, head groups, sterol content, and membrane-associated proteins. Therefore, an increase or decrease in a given lipid or protein species cannot be directly translated into a predictable change in membrane fluidity without additional biophysical validation. This point is further supported by our observation that knockdown of genes involved in both sphingolipid biosynthesis and sphingolipid degradation increased endolysosomal membrane rigidity. These perturbations would be expected to affect lipid composition in different, possibly even opposing, ways, making it unlikely that the shared rigidification phenotype is caused by accumulation or depletion of one single lipid species. Rather, distinct lipidomic changes may converge on a common biophysical outcome: reduced endolysosomal membrane fluidity.

We have clarified this point in the Discussion and now state that future lysosome-enriched or organelle-specific lipidomic/proteomic approaches should be combined with direct manipulation of candidate lipid or protein species, followed by measurements of membrane fluidity and rupture, to determine which changes causally contribute to endolysosomal membrane rigidification. Such experiments would address the distinct question of which molecular components mediate the effect. By contrast, the central aim of the present study was to test whether genetic perturbation of enzymes involved in sphingolipid metabolism alters membrane fluidity and thereby promotes endolysosomal rupture and tau seeding.

For this question, direct biophysical measurements of membrane fluidity and quantitative readouts of membrane rupture are the most relevant assays. We therefore used complementary quantitative approaches in two distinct model systems: FRAP of the lysosomal membrane protein LAAT-1::mCherry in *C. elegans* and C-Laurdan GP imaging in human cells. The fact that perturbing sphingolipid metabolism reduced endolysosomal membrane fluidity in *C. elegans* and increased lysosome-associated membrane rigidity in human cells supports the robustness and reproducibility of the central conclusion across independent model systems. In the revised manuscript, we further strengthened the human-cell data by adding SH-SY5Y neuroblastoma cells as a neuronal-like model and by combining C-Laurdan imaging with LysoTracker-based analysis to assess lysosome-associated membrane properties.

To further address causality, we manipulated membrane fluidity independently of sphingolipid metabolism enzymes using fatty acid supplementation. Increasing membrane rigidity with PA exacerbated tau-induced endolysosomal rupture and seeded aggregation, whereas increasing membrane fluidity with ALA reduced tau-induced membrane rigidification, endolysosomal rupture, and seeded aggregation. Thus, the revised manuscript combines genetic perturbation of sphingolipid metabolism, quantitative membrane-fluidity measurements, whole-cell and lysosome-associated C-Laurdan analysis, and Galectin-based rupture assays across complementary models.

Regarding lysosomal function, we agree that functional readouts are informative, but lysosomal membrane rupture and global lysosomal degradative capacity are related but not identical readouts. This distinction is supported by Yong et al., who reported that lipid dysregulation can induce lysosomal membrane permeabilization and lysosomal accumulation of endogenous protein aggregates without broadly impairing core lysosomal or proteasomal functions [2]. Accordingly, the absence of overt defects in general lysosomal activity would not necessarily exclude membrane damage.

> *The human cell experiments were performed exclusively in HEK293T cells, which are not physiologically relevant for modeling Alzheimer's disease or lysosomal function in*

> *neurons. Given that the study aims to draw conclusions related to tau aggregation and lysosomal membrane integrity, the use of a more disease relevant cellular model is essential. There are several established AD-relevant cell models, including iPSCderived neurons, neuroblastoma lines expressing tau, or microglial models, which would better reflect the cellular context of tauopathies. Validation of key findings in at least one of these systems would substantially enhance the biological relevance and translational impact of the study.*

We have expanded and clarified the human cell data in the revised manuscript. Specifically, we now include SH-SY5Y human neuroblastoma cells for key C-Laurdan experiments assessing membrane rigidity after SPHK2 knockdown. We also show that recombinant tau fibrils increased membrane rigidity in SHSY5Y and HEK293T cells, including in LysoTracker-positive compartments.

Importantly, the HEK293T cells are used for specific, established quantitative assays rather than as a model of neuronal toxicity. In particular, HEK293T sfGFP-LGALS3 cells are used to quantify galectin puncta formation as a readout of endolysosomal rupture, and HEK tau-Venus biosensor cells are used to quantify seeded tau aggregation. Thus, SH-SY5Y cells and HEK293T cells are used for complementary purposes: SHSY5Y cells provide a more neuronal-like human cell context for membrane-rigidity measurements, whereas HEK293T reporter/biosensor cells provide robust quantitative assays for galectin puncta formation and tau seeding.

In addition, tau-associated neuronal dysfunction and toxicity were assessed *in vivo*, in functional *C. elegans* touch receptor neurons. In the revised manuscript, we show that ALA supplementation mitigated the age-dependent touch-response deficit and reduced neurotoxicity in animals expressing F3ΔK281::mCherry in touch receptor neurons. We have also revised the wording throughout the manuscript to avoid implying that HEK293T cells are used to model neuronal toxicity.

Finally, the relevance of these hits to human neuronal tau seeding is also supported by our previous study, in which conserved hits from the *C. elegans* screen, including sphingosine kinase perturbation, were validated in human iPSC-derived neurons for their effect on seeded tau aggregation [1]. We now cite this published study where appropriate. Together, the revised manuscript combines neuronal-like human SH-SY5Y cells, established HEK293T tau-seeding and galectin reporter assays, *in vivo* neuronal readouts in *C. elegans*, and prior validation in human iPSC-derived neurons, thereby strengthening the biological relevance of the conclusions while using each model for the assay in which it is most informative.

> *The authors reported that PUFA supplementation rescues neurotoxic phenotypes by increasing membrane fluidity. However, the data supporting this claim rely entirely on confocal imaging, shown in both the main and supplemental figures. To substantiate the mechanistic link between PUFA treatment and improved lysosomal membrane properties, the authors should include functional assays demonstrating that PUFAs are indeed incorporated into lysosomal membranes. Additionally, lipidomics analysis would be valuable to identify which lipid species are altered upon supplementation and correlate these changes with the observed phenotypic rescue. Furthermore, the conclusion that PUFAs rescue "neurotoxic phenotypes" is not appropriate based on data derived solely from HEK293T cells, which are not neuronal. To make claims about tau-related neurotoxicity, the authors should validate their findings in a more relevant neuronal model, such as SH-SY5Y neuroblastoma cells expressing tau or iPSC-derived neurons. This would better reflect the cellular environment of Alzheimer's disease and provide stronger support for the proposed therapeutic potential of PUFA supplementation.*

We agree that PUFA supplementation can have effects beyond membrane fluidity and that our data do not directly demonstrate incorporation of ALA into lysosomal membranes. We have therefore revised the Discussion to explicitly acknowledge this limitation. In the revised text, we state that "PUFAs can also influence lipid signaling, oxidative stress responses, and broader membrane remodeling" and that we "cannot exclude additional direct or indirect effects of ALA." At the same time, we note that the opposing effects of PA and ALA, together with the sphingolipid-metabolism knockdown data, support membrane fluidity as a major determinant of endolysosomal membrane integrity and rupture in our models. To strengthen the link between ALA and lysosome-associated membrane properties, we combined CLaurdan imaging with LysoTracker-based analysis. In the revised Results, we show that ALA prevented tau-induced membrane rigidification and that LysoTracker-based analysis indicated effects on lysosome-associated membrane properties. ALA also reduced tau-induced endolysosomal rupture and seeded aggregation in human cell models.

Regarding lipidomics, we refer to our response above and to the revised Discussion. We agree that lipidomics would be valuable to identify ALA-induced lipid changes, but such data would not by itself establish how these changes affect membrane fluidity without additional biophysical validation.

Finally, we clarify that our conclusion regarding tau-associated neuronal dysfunction and toxicity is not based on HEK293T cells. HEK293T cells were used for established quantitative assays of Galectin puncta formation and seeded tau aggregation. The neurotoxicity experiments were performed *in vivo* in *C. elegans* touch receptor neurons, where ALA supplementation reduced galectin foci formation, mitigated age-dependent touch-response deficit and reduced neuronal toxicity.

> *While the authors demonstrate that ALA supplementation mitigates neurotoxicity in C. elegans expressing aggregated tau (F3ΔK281::mCherry), the current data are not sufficient to conclude that ALA directly rescues tau aggregation toxicity via a lysosome-specific mechanism. It remains unclear how lipid composition is altered upon ALA treatment and whether these changes correlate with functional improvement of lysosomal pathways. The manuscript does not provide mechanistic insight into how ALA enhances lysosomal health or attenuates endolysosomal damage. Moreover, supplementation with PUFAs like ALA can activate a wide range of cellular processes beyond lysosomal function, including alterations in membrane fluidity, signaling cascades, and oxidative stress responses. The authors should clarify how they distinguish the lysosome-related effects from these alternative pathways. For example, did they observe specific lysosomal markers or structural improvements in lysosomes upon ALA treatment?*
>
> *Additional data or controls would be necessary to support a lysosome-specific protective mechanism and to exclude the involvement of other PUFA-responsive pathways in the observed phenotypes.*

We agree that our data do not prove that ALA acts exclusively through a lysosome-specific mechanism or that ALA is directly incorporated into lysosomal membranes. We have therefore revised the manuscript to avoid this interpretation and explicitly acknowledge alternative PUFA-responsive pathways. In the revised Discussion, we state that "PUFAs can also influence lipid signaling, oxidative stress responses, and broader membrane remodeling" and that we "cannot exclude additional direct or indirect effects of ALA." We further conclude more cautiously that the opposing effects of PA and ALA, together with the sphingolipid metabolism perturbation data, support membrane fluidity as a major determinant of endolysosomal membrane integrity and rupture in our models.

To strengthen the lysosome-related aspect of the mechanism, we added LysoTracker-based analysis to the C-Laurdan experiments. In the revised Results, ALA prevented tau-induced membrane rigidification, and LysoTracker-based analysis indicated that ALA also affected lysosome-associated membrane properties. ALA further reduced tau-induced Galectin puncta formation and seeded tau aggregation in human cell models. These data support an effect of ALA on lysosome-associated membrane order and rupture, while not excluding additional effects through lipid signaling, oxidative stress responses, or other PUFA-responsive pathways.

Regarding lipid composition, we refer to the revised Discussion and our response above. We agree that lipidomics would be valuable to identify ALA-induced lipid changes, but such analyses would need to be organelle-specific and combined with biophysical validation to determine how candidate lipid changes affect membrane fluidity and rupture.

Finally, we clarify that our conclusion regarding tau-associated neuronal dysfunction and toxicity is based on the *C. elegans* experiments, not on HEK293T cells. HEK293T cells were used for quantitative Galectin puncta and tau-seeding assays, whereas neuronal dysfunction and toxicity were assessed *in vivo* in touch receptor neurons in *C. elegans*. In the revised Results, we state that ALA supplementation mitigated galectin foci formation, age-dependent touch-response deficit and reduced neuronal toxicity in animals expressing F3ΔK281::mCherry in these neurons.

> ***Reviewer #2 (Public review):***
>
> *Tittelmeier et al. investigated the role of sphingolipid (SL) metabolism in the maintenance of endolysosomal vesicle integrity. They find that both impaired SL biosynthesis and degradation in C. elegans, decrease the fluidity of endolysosomal membranes and promote their rupture, while it has little effect on plasma membrane fluidity. Endolysosomal membrane fluidity is also negatively affected in human cells upon knockdown (KD) of a gene (SPHK2) involved in the SL degradation pathway. Aggregated forms of tau in both models (C. elegans and human cells) can also cause rigidification of the endolysosomal membrane, with SL homeostasis disruption having an additive effect, exacerbating endolysosomal rupture. Notably, KD of SPHK2 also increased the formation of tau foci, suggesting that compromised endolysosomal integrity may promote tau aggregation. These data provide a clearer understanding of how genetic manipulation of SL metabolism affects endolysosomal membranes and their rigidification in the context of tau aggregation. Supplementation of polyunsaturated fatty acids (PUFAs), which has a beneficial effect on Alzheimer's patients, improved membrane fluidity and reduced tau propagation in human cells and tau-associated neurotoxicity in C. elegans, suggesting a possible mechanism of action.*
>
> *Overall, the conclusions of this paper are supported by the data, with a few aspects requiring further clarification and elaboration.*
>
> *(1) A reference to Figure S2E-G, which shows that KD of SL biosynthesis genes do not affect the plasma membrane, is missing from the main text.*

We thank the reviewer for pointing this out. We have added the reference to the respective figures in the main text when discussing the plasma membrane FRAP experiments.

> *(2) In Figure 3C, lipofectamine alone shows that it increases membrane rigidity (increased GP values), not membrane fluidity.*

We thank the reviewer for pointing out this incorrect wording. A higher GP index indicates increased membrane order/rigidity, not increased membrane fluidity. Since the revised main figure now includes the SH-SY5Y data, in which Lipofectamine alone did not significantly

alter GP values, we removed the misleading statement from the Results. Importantly, all siRNA-mediated knockdown experiments were compared to matched control siRNA conditions exposed to the same transfection reagent. Thus, the effect attributed to SPHK2 KD is assessed relative to the appropriate Lipofectamine-containing control condition.

> *(3) In Figure 3F, the EV cntl condition expressing F3:mCh tau should have increased LGALS3 foci compared to the mCh EV cntl according to Ref (20) and its Figure 2G (at least for Day 5 animals), which would be indicative of the tau spreading in hypodermal tissue. What C. elegans age was examined in Figure 3F? Can the authors provide evidence of the transmission of the F3:mCh tau from the touch receptor neurons to the hypodermis in the EV [similar to Figure 2C & D from Ref (20)] and compare it to the KDs? Otherwise, it seems that KD of SL genes impacts not only endolysosomal rupture but significantly affects tau accumulation/spreading as well (e.g., shown later in HEK cells, where SPHK2 KD increases the formation of tau-Venus foci).*

We thank the reviewer for raising this important point. The analysis referred to by the reviewer has now been moved to the revised *C. elegans* section and is presented as Figure 4A and B. The experiments were performed in the reporter strain used in our genome-wide screen In Ref (20), now published in Autophagy [1]. We clarified the purpose of the reporter strain and the relationship between tau transmission and the galectin puncta readout. In the revised manuscript, we now state: “In this strain, endolysosomal membrane damage is monitored in the hypodermis by expression of human galectin-3 fused to superfolder-GFP (sfGFP::LGALS3). The animals also express an aggregation-prone tau fragment fused to mCherry (F3ΔK281::mCherry) in touch receptor neurons, which is transmitted to the hypodermis, as described previously [20].” We further clarify that sfGFP::LGALS3 puncta formation, not F3ΔK281::mCherry, is the readout of endolysosomal rupture: “Under steady-state conditions, sfGFP::LGALS3 remains diffusely distributed throughout the cytosol. Upon endolysosomal damage, luminal β-galactosides become exposed and recruit sfGFP::LGALS3 into visible puncta, providing a sensitive readout of vesicle rupture”.

Furthermore, we now better explain that transmitted tau sensitizes endolysosomal membranes to additional perturbations rather than necessarily inducing a strong lysosomal rupture phenotype on its own. In the experiments shown in Figure 4A and B, we compare F3ΔK281::mCherry animals with matched mCherry-only control animals that also express sfGFP::LGALS3 in the hypodermis. We now state: “We compared animals expressing F3ΔK281::mCherry in touch receptor neurons, from where it is transmitted to the hypodermis, with matched controls expressing mCherry alone in the same neurons. In both strains, sfGFP::LGALS3 is expressed in the hypodermis to monitor endolysosomal membrane damage.” We have also clarified the age of the animals in the revised figure legends.

To experimentally address whether the enhanced rupture phenotype could be explained by altered tau transmission, we quantified hypodermal F3ΔK281::mCherry levels after *sphk-1* RNAi (new Figure 4C, D). Importantly, *sphk-1* RNAi did not increase hypodermal F3ΔK281::mCherry levels, arguing that the enhanced rupture phenotype is not due to increased tau transmission. Moreover, *C. elegans* neurons are largely refractory to systemic RNAi under the conditions used here [3]. We have added this important information to the Discussion. Specifically, the revised manuscript states that “the enhanced rupture phenotype is unlikely to result from a direct effect of RNAi on neuronal F3ΔK281::mCherry expression, as *C. elegans* neurons are largely refractory to systemic RNAi under the conditions used here,” supporting the interpretation that the RNAi treatments primarily affect endolysosomal integrity in the recipient tissue rather than neuronal tau expression itself.

Finally, we would like to clarify that the increased tau-Venus foci in HEK cells should not be interpreted as a direct induction of tau aggregation by SPHK2 KD. Only upon addition of recombinant tau fibrils did SPHK2 KD significantly increase tau-Venus foci formation (Figure 3 H, I). This is consistent with the control experiments performed in human iPSCs in our

previous study and supports our interpretation that perturbation of sphingolipid metabolism increases susceptibility to seeded tau aggregation by promoting endolysosomal rupture and tau seed escape, rather than by directly increasing tau aggregation or tau transmission.

> *(4) Sphingolipids are essential membrane components and signaling molecules. Does KD of SL genes in C. elegans and the subsequent endolysosomal rupture cause any major, intermediate, or minor defects/phenotypes (in non-aggregation prone models, w/t.)?*

We agree that sphingolipids are essential membrane components and signaling molecules and that perturbing sphingolipid metabolism can have broader physiological consequences. In the revised manuscript, we address this point in two ways.

First, we directly tested whether SL gene knockdown can induce endolysosomal rupture independently of aggregation-prone tau by using matched control animals expressing mCherry alone in touch receptor neurons while also expressing sfGFP::LGALS3 in the hypodermis. In these animals, knockdown of most SL-related hits resulted in nearly all animals displaying hypodermal sfGFP::LGALS3 foci, indicating that perturbation of SL metabolism can compromise endolysosomal integrity in the absence of transmitted F3ΔK281::mCherry (Figure 4A, B).

Second, we have added a Discussion paragraph to place these findings into a broader physiological context. We now clarify that endolysosomal membrane rupture and global lysosomal function are related but not identical readouts. In support of this distinction, we discuss work showing that lipid dysregulation can induce lysosomal membrane permeabilization and lysosomal accumulation of endogenous protein aggregates without broadly impairing core lysosomal or proteasomal function [2]. Thus, membrane damage can occur even when general lysosomal activity is not overtly disrupted.

We also discuss a recent study published during the revision of this manuscript that independently identified SPHK-1 as an important regulator of lysosomal integrity in *C. elegans*, showing that strong *sphk1* loss-of-function causes lysosomal sphingosine accumulation, membrane rupture, impaired degradative function, cargo accumulation, developmental defects, and reduced lifespan [4].

Importantly, while that study focused on a strong loss-of-function mutation in a single SL-metabolism gene, our data show that knockdown of multiple SL-metabolism genes, including genes involved in both SL biosynthesis and degradation, converges on reduced endolysosomal membrane fluidity and increased rupture. This suggests that the observed membrane rigidification and rupture are not specific to one mutant background but represent a broader consequence of perturbing SL metabolism at multiple points. A systematic characterization of all organismal phenotypes caused by each SL gene knockdown was beyond the scope of the present study. Therefore, the revised manuscript now makes clear that the study focuses on endolysosomal membrane fluidity and rupture because these membrane-level changes are directly linked to tau seed escape and seeded tau aggregation, while broader physiological consequences may vary depending on the strength and context of the perturbation.

> ***Reviewer #3 (Public review):***
>
> *Summary:*
>
> *The authors set off with an analysis of the lysosomal integrity upon knockdown of genes of the sphingolipid metabolic pathway that they identified in a previous (yet unpublished) work of an RNA screen using a new C. elegans Tau model. They then used cell culture and C. elegans experiments to study the link between lysosomal rupture and Tau propagation.*

> *Strengths:*
>
> *The authors use two complementary model systems and use probes to assess membrane rigidity that allow a quick assessment of the membrane dynamics and offer the opportunity to treat the cells with lipids, RNAi. Tau seeds, etc.*
>
> *Weaknesses:*
>
> *The main weakness is that this work builds on not-yet-peer-reviewed manuscript that established a new C. elegans Tau model and RNAi screen that aimed to identify genes involved in the propagation of Tau.*
>
> *This reviewer misses essential information of the C. elegans Tau strain (not included in the method section): e.g., promoter used for the expression, information on the used Tau variant, expression pattern, and aggregation, etc.*

We thank the reviewer for raising this point. The related study establishing the *C. elegans* tau transmission model and RNAi screen has now been peer-reviewed and published in Autophagy [1]. We now cite the published article throughout the revised manuscript instead of the previous preprint.

We also agree that the current manuscript should be understandable without requiring the reader to consult the previous paper for the basic logic of the model. We therefore added a clearer introduction of the reporter strain in the Results. Specifically, we now explain that the strain expresses the aggregation-prone tau fragment F3ΔK281::mCherry in touch receptor neurons, that this tau fragment is transmitted to the hypodermis, and that endolysosomal membrane damage is monitored in the hypodermis using sfGFP::LGALS3. We further clarify that sfGFP::LGALS3 remains diffuse under steady-state conditions and forms puncta upon endolysosomal membrane damage, when luminal β-galactosides become exposed. Thus, the revised manuscript now provides the key information needed to understand the experimental system used here, while the published Autophagy paper is cited for the full characterization of the tau transmission model, expression pattern, aggregation properties, and original genome-wide RNAi screen.

> *Throughout the study, I missed data on:*
>
> *(1) Effect of the knockdown on Tau expression, localisation (with lysosomal membrane?), aggregation, and proteotoxicity. The effect of the RNAi-mediated knockdown could also simply lead to a reduced expression of Tau that, in turn, leads to suppressed propagation.*

We agree that it is important to distinguish effects on tau expression/transmission from effects on endolysosomal membrane integrity. In the *C. elegans* experiments, F3ΔK281::mCherry is expressed in touch receptor neurons and transmitted to the hypodermis, where sfGFP::LGALS3 reports endolysosomal membrane damage. We now describe this more clearly in the revised Results.

The RNAi treatments target genes involved in sphingolipid metabolism under systemic RNAi conditions. Because *C. elegans* neurons are largely refractory to systemic RNAi in the absence of sensitizing backgrounds [3], which we did not use, a direct RNAi-mediated reduction of neuronal F3ΔK281::mCherry expression is very unlikely. We have added this point to the Discussion, stating that “the enhanced rupture phenotype is unlikely to result from a direct effect of RNAi on neuronal F3ΔK281::mCherry expression, as *C. elegans* neurons are largely refractory to systemic RNAi under the conditions used here.”

Experimentally, we also tested whether sphingolipid perturbation alters transmitted tau levels (new Figure 4C, D). Specifically, we quantified hypodermal F3ΔK281::mCherry after

sphk-1 RNAi and found no increase, arguing that the enhanced rupture phenotype is not due to increased tau transmission.

Moreover, in the cell-based tau-Venus assay, SPHK2 knockdown alone did not induce detectable tau aggregation in the absence of exogenously added tau fibrils (Figure 3H, I). Only upon addition of recombinant tau fibrils did SPHK2 knockdown significantly increase tau-Venus foci formation. We now state this explicitly in the revised Results and conclude that disruption of sphingolipid metabolism is not sufficient on its own to initiate detectable tau aggregation under the conditions tested here but rather increases cellular susceptibility to seeded tau aggregation when tau fibrils are present.

Together, these data argue against a direct effect of sphingolipid gene knockdown on tau expression or spontaneous tau aggregation. Instead, they support our interpretation that perturbation of sphingolipid metabolism compromises endolysosomal membrane integrity, thereby facilitating tau seed escape and seeded aggregation when tau seeds are present.

> *(2) A quantification of RNAi knockdown is needed to judge the efficiency of the RNAi, in particular for the combinatorial RNAi experiments involving 2 and even 4 genes in parallel. Ideally, these analyses should be validated with mutants for these genes.*

We agree that RNAi efficiency can vary between clones and that this is particularly relevant for combinatorial RNAi experiments targeting two or more potentially redundant genes. We have added this limitation to the Results section and now state: “Because KD efficiency was not assessed for the individual RNAi clones or co-RNAi combinations, these experiments do not allow comparison of relative RNAi strength or inference of the relative importance of individual genes. Thus, the conclusions drawn from these RNAi experiments are qualitative: specific single or combined KDs can promote endolysosomal rupture, whereas the absence of a detectable phenotype after RNAi cannot exclude gene involvement, as KD may have been insufficient.”

Where mutant strains were available, we performed genetic validation. Specifically, a *sphk-1* mutant available at CGC (CZ24969; *sphk-1*(*ju831*)) also showed increased hypodermal sfGFP::LGALS3 puncta (new Figure S1A), supporting the RNAi-based conclusion that genetic perturbation of sphingolipid metabolism compromises endolysosomal integrity. Corresponding mutant strains were not available for the other selected hits. Importantly, most hits also induced sfGFP::LGALS3 foci in human HEK293T cells as assessed in our previous study [1], providing additional support that the observed effects are not random RNAi artifacts.

> *Further:*
>
> *(3) Figure 4 H, I: Would Tau also aggregate in the absence of externally added Tau?*

No. In the tau-Venus biosensor cell line, *SPHK2* knockdown alone did not increase tau-Venus foci formation (now Figure 3H, I). Tau-Venus foci increased only after addition of recombinant tau fibrils and were further enhanced by *SPHK2* knockdown. We now state this explicitly in the Results.

> *(4) How specific is the effect for Tau? It would help if the authors could assess other amyloid proteins.*

We agree that similar membrane-level mechanisms may apply to other amyloid assemblies. We have therefore added recent literature to the Discussion supporting the broader concept that intralysosomal amyloid assemblies can physically deform and rupture lysosomal membranes. The revised manuscript states: “This interpretation is consistent with recent ultrastructural studies showing that intralysosomal amyloid assemblies can physically deform and rupture lysosomal membranes.” We further clarify that “whether this

mechanism is specific to tau or also applies to other amyloid assemblies remains to be determined."

Whether perturbation of SL metabolism similarly affects endolysosomal escape and seeded aggregation of other disease-associated amyloid proteins is an important question that we plan to address in future work. However, these experiments require additional disease-specific models, aggregation assays, and validation, and are therefore beyond the scope of the present revision.

> *(5) The connection between sphingolipids and AD is not new. See He et al, 2010, Neurobiol. Aging + numerous publications and also not between Tau seeding and lysosomal rupture: Rose et al., PNAS 2024 (that has been cited by the authors).*

We agree and our manuscript does not aim to establish these associations as new. We state explicitly that alterations in sphingolipid metabolism have been reported in aging and AD, and that endolysosomal rupture is increasingly recognized as a critical step in tau seed escape and propagation.

The novelty of our study lies in mechanistically connecting these two previously established areas. Specifically, we show that genetic perturbation of enzymes involved in sphingolipid metabolism reduces endolysosomal membrane fluidity, promotes membrane rupture, and thereby increases susceptibility to tau seed escape and seeded aggregation. We have revised the Introduction and Discussion to better emphasize this mechanistic contribution.

> ***Recommendations for the authors:***
>
> ***Reviewer #1 (Recommendations for the authors):***
>
> *Figure formatting and annotation need improvement. Panel letters throughout the figures should be in uppercase, and gene names in pathway diagrams should be italicized for consistency. Several scale bars are missing, including in Figures 1C, 2A, and 2H, and should be clearly indicated in the figures and legends. In Figure 1C, the age of the worms used in the assay is not specified. While the Methods section mentions "age-synchronized animals," the precise age at the time of imaging or experimentation is not stated. It would strengthen the study to explore whether membrane integrity phenotypes vary between young adults (day 1) and older adults (day 7 or 10) across the different conditions. Figure 1B lacks sufficient detail describing the galectin puncta assay used. A brief explanation of the assay rationale and readout would help contextualize the findings.*

We thank the reviewer for pointing this out. We have revised the figures and figure legends accordingly by standardizing panel labels, adding scale bars where missing, and providing the age of animals used in the assays. We also expanded the description of the galectin puncta assay in the Results to explain the rationale and readout of sfGFP::LGALS3 puncta formation.

Regarding the reviewer's suggestion to compare young and aged animals, we agree that age-dependent changes in endolysosomal membrane integrity are an interesting question. However, the purpose of the present study was to investigate how perturbation of sphingolipid metabolism affects endolysosomal membrane fluidity and rupture under the assay conditions used in our original screen. A systematic comparison across aging is beyond the scope of the current revision. We have therefore clarified the animal ages used in the relevant figure legends and Methods.

> *In Figure S1A, the authors show co-knockdown of multiple genes, including one condition with simultaneous RNAi against four targets. Because different RNAi clones can vary in knockdown efficiency, it is important to provide validation of gene knockdown levels (e.g., by qRT-PCR) shown in both panels a and b.*

We agree that RNAi efficiency can vary between clones and that this is particularly relevant for combinatorial RNAi experiments targeting two or more potentially redundant genes. We have added this limitation to the Results section and now state: “Because KD efficiency was not assessed for the individual RNAi clones or co-RNAi combinations, these experiments do not allow comparison of relative RNAi strength or inference of the relative importance of individual genes. Thus, the conclusions drawn from these RNAi experiments are qualitative: specific single or combined KDs can promote endolysosomal rupture, whereas the absence of a detectable phenotype after RNAi cannot exclude gene involvement, as KD may have been insufficient.”

Where mutant strains were available, we performed genetic validation. Specifically, a *sphk-1* mutant available at CGC (CZ24969; *sphk-1*(*ju831*)) also showed increased hypodermal sfGFP::LGALS3 puncta (new Figure S1A), supporting the RNAi-based conclusion that genetic perturbation of sphingolipid metabolism compromises endolysosomal integrity. Corresponding mutant strains were not available for the other selected hits. Importantly, most hits also induced sfGFP::LGALS3 foci in human HEK293T cells as assessed in our previous study [1], providing additional support that the observed effects are not random RNAi artifacts.

> *In Figure 2E, the FRAP recovery curves show only ~60% recovery in controls after 25 seconds, and an even lower recovery (~40%) in hpo-8 and spp-10 RNAi conditions. The authors should discuss why the recovery is incomplete and what it implies about the mobile fraction of the protein or membrane components in these conditions.*

We agree that incomplete FRAP recovery is informative. For this reason, we report both the time to half-maximal recovery (thalf) and the maximal recoverable fluorescence signal. Increased thalf indicates reduced lateral mobility of LAAT-1::mCherry within the lysosomal membrane, consistent with reduced membrane fluidity. In addition, a reduced maximal recovery suggests that a larger fraction of the reporter is immobile or only slowly mobile during the time window analyzed. This may reflect stronger confinement of LAAT-1::mCherry within even more rigid membrane domains. However, because RNAi efficiency may differ between clones and we have not assessed their individual KD efficiency, we avoid overinterpreting differences in the absolute strength of recovery defects between individual KDs. Instead, we conclude that KD of sphingolipid-metabolism genes identified in our screen consistently reduces lysosomal membrane fluidity, as reflected by increased thalf and, in some cases, reduced maximal recovery.

> *In Figure S3A, the Western blot for SPHK2 shows unequal loading between the control and siSPHK2 lanes. The blot should be normalized to a loading control and quantified to demonstrate knockdown efficiency.*

We have quantified SPHK2 levels relative to GAPDH across independent experiments and present the normalized quantification (Figure S3C-E).

> *Key experimental details are missing from the manuscript. The strains of C. elegans and RNAi bacteria used were not described, and there is no information on biological replicates. The authors should clarify how many times each experiment was performed and provide more transparency on experimental reproducibility.*

We thank the reviewer for pointing this out. The *C. elegans* strains and RNAi bacterial clones used in this study were established and fully described in our previous study, which has now been published in Autophagy [1]. We now cite the published article throughout the revised manuscript and have added additional information in the Results section to explain the key features of the strains used here.

We have also revised the Methods and figure legends to improve transparency regarding experimental details. The figure legends include the number of biological replicates, the number of animals or cells analyzed, and the statistical tests used for each experiment. In addition, the Statistical Analysis section in the Methods now summarizes how replicate numbers and sample sizes are reported across the study. Finally, the source details for the strains and RNAi clones used in this study are now provided in Tables S1 and S2, respectively. These revisions should improve the experimental clarity and reproducibility of the data shown.

References:

(1) Sandhof CA, Martin N, Tittelmeier J, Schlueter A, Pezzali M, Schoendorf DC, et al. A novel C. elegans model for MAPT/Tau spreading reveals genes critical for endolysosomal integrity and seeded MAPT/Tau aggregation. Autophagy. 2025;21(12):2963-81. Epub 20250904. doi: 10.1080/15548627.2025.2551676. PubMed PMID: 40851193; PubMed Central PMCID: PMCPMC12758218.

(2) Yong J, Villalta JE, Vu N, Kukurugya MA, Olsson N, Lopez MP, et al. Impairment of lipid homeostasis causes lysosomal accumulation of endogenous protein aggregates through ESCRT disruption. eLife. 2024;12. Epub 20241223. doi: 10.7554/eLife.86194. PubMed PMID: 39713930; PubMed Central PMCID: PMCPMC11666243.

(3) Calixto A, Chelur D, Topalidou I, Chen X, Chalfie M. Enhanced neuronal RNAi in C. elegans using SID-1. Nat Methods. 2010;7(7):554-9. doi: 10.1038/nmeth.1463. PubMed PMID: 20512143; PubMed Central PMCID: PMC2894993.

(4) Li Y, Zhang J, Li M, Yang L, Wang X. Sphingosine kinase SPHK-1 maintains sphingolipid metabolism to protect lysosome membrane integrity in C. elegans. Mol Biol Cell. 2026;37(1):ar1. Epub 20251105. doi: 10.1091/mbc.E25-04-0182. PubMed PMID: 41191545; PubMed Central PMCID: PMCPMC12696880.

https://doi.org/10.7554/eLife.106865.2.sa0